A simple photometric factor in perceived depth order of bistable transparency patterns

Taiki Fukiage Graduate School of Interdisciplinary Information Studies, University of Tokyo, Meguro-ku, Tokyo, Japan

Takeshi Oishi Institute of Industrial Science, University of Tokyo, Meguro-ku, Tokyo, Japan

Katsushi Ikeuchi Interfaculty Initiative in Information Studies, University of Tokyo, Meguro-ku, Tokyo, Japan

Previous studies on perceptual transparency defined the photometric condition in which perceived depth ordering between two surfaces becomes ambiguous. Even under this bistable transparency condition, it is known that depth-order perceptions are often biased toward one specific interpretation (Beck, Prazdny, & Ivry, 1984; Delogu, Fedorov, Belardinelli, & van Leeuwen, 2010; Kitaoka, 2005; Oyama & Nakahara, 1960). In this study, we examined what determines the perceived depth ordering for bistable transparency patterns using stimuli that simulated two partially overlapping disks resulting in four regions: *a* (background), *b* (portion of right disk), *p* (portion of left disk), and *q* (shared region). In contrast to the previous theory that proposed contributions of contrast against the background region (i.e., contrast at contour *b*/*a* and contrast at contour *p*/*a*) to perceived depth order in bistable transparency patterns, the present study demonstrated that contrast against the background region has little influence on perceived depth order compared with contrast against the shared region (i.e., contrast at contour *b*/*q* and contrast at contour *p*/*q*). In addition, we found that the perceived depth ordering is well predicted by a simpler model that takes into consideration only relative size of lightness difference against the shared region. Specifically, the probability that the left disk is perceived as being in front is proportional to $(|b-q|-|p-q|)\,/\,(|b-q|+|p-q|)$ calculated based on lightness.

Introduction

Classification of perceptual transparency based on Adelson-Anandan-Anderson's contrast polarity rule

The human visual system decomposes a two-dimensional retinal image in the same location into two surfaces at different depths, even when a very simple pattern is presented. One of the major issues in this "perceptual transparency" is what photometric condition is important for the depth stratification. Regarding this problem, Adelson and Anandan (1990) and Anderson (1997) proposed that the luminance pattern around an X-junction (a junction where four regions meet together) plays the main role in perceptual transparency and argued that the perceived state of the surface decomposition depends on categories of the X-junction. They classified X-junctions into three categories according to polarity relationships of aligned contours: nonreversing junction, single-reversing junction, and double-reversing junction. For example, the X-junction in Figure 1A is classified as a single-reversing junction since contrast polarity along vertical contours is reversed while contrast polarity along horizontal contours is preserved (see the magnified X-junction in Figure 1A). In this case, the surface comprising regions p and q (the bottom-left square) is always perceived as transparent and being in front according to their theory. This special case induced by the single-reversing junction was thus termed unique transparency. On the other hand, the X-junction in Figure 1B is classified as a nonreversing junction since contrast polarity along both horizontal and vertical

Citation: Fukiage, T., Oishi, T., & Ikeuchi, K. (2014). A simple photometric factor in perceived depth order of bistable transparency patterns. *Journal of Vision, 14*(5):2, 1–27, http://www.journalofvision.org/content/14/5/2, doi:10.1167/14.5.2.

doi: 10.1167/14.5.2 Received May 20, 2013; published May 5, 2014 ISSN 1534-7362

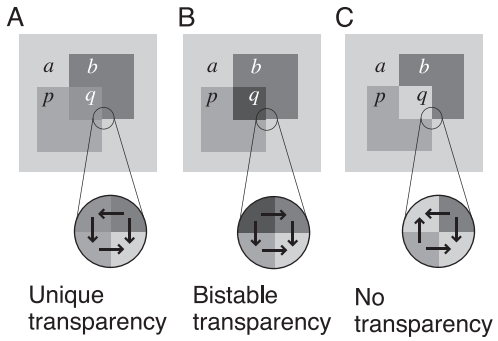

Figure 1. Schematic explanation of the Adelson-Anandan-Anderson contrast polarity rule. (A) Single-reversing X-junction induces unique transparency, in which the same surface (in this case, surface *pq*) is always perceived as transparent and being in front of the other surface. (B) Nonreversing X-junction induces bistable transparency, in which a surface comprising any pair of two adjacent regions can be perceived as transparent and in front. (C) Double-reversing junction does not induce perceptual transparency.

contours is preserved. In this case, it remains ambiguous which surface is perceived as being in front; sometimes the bottom-left square may appear to be transparent and in front, but sometimes the top-right square may appear to be transparent and in front. Thus, the perceptual transparency under this condition was termed bistable transparency. Strictly speaking, in the case of a nonreversing junction, the surface comprising regions *a* and *p* or the surface comprising regions *a* and *b* can also appear to be transparent and in front, but figural constraints, such as inclusion, restrict perceived interpretations to the two alternatives mentioned first. (The visual system prefers smallish, coherent objects to smallish holes in larger objects; see Koenderink, van Doorn, Pont, & Richards, 2008.) Finally, the X-junction in Figure 1C is classified as a double-reversing junction since contrast polarity along both horizontal and vertical contours is reversed. For the double-reversing junction, one barely experiences transparency perception.

The Adelson-Anandan-Anderson contrast polarity rule has also been validated from an ecological viewpoint using a physical model of transparency (Adelson & Anandan, 1990; Kitaoka, 2005). Although there are a lot of models to describe transparency, the most influential and classical model is the one proposed by Metelli. Metelli (1974a, 1974b, 1985) used an episcotister (a disk with an open sector) to simulate a transparent layer. When the episcotister is rotated above the critical flicker frequency (Figure 2A), the disk appears to be a transparent layer (Figure 2C). If the angular proportion of the open sector is *t*, the transmittance of the simulated transparent layer can be regarded as *t*. Under this assumption, the reflectance of the regions *p* and *q* can be described as follows using

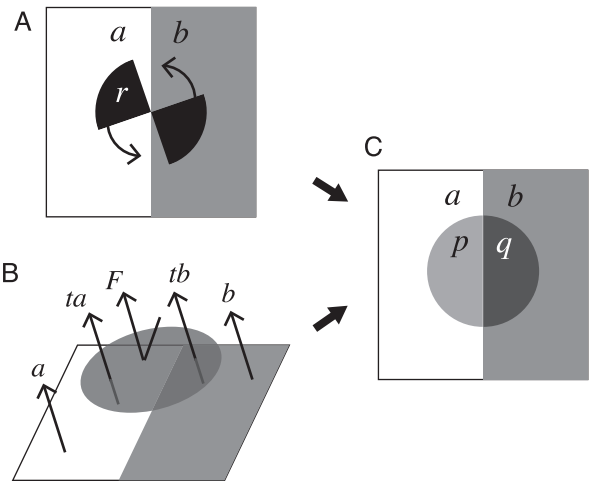

Figure 2. Physical configurations used in (A) Metelli's model and (B) Gerbino's model, and (C) the resultant transparency pattern.

the reflectance of the background regions *a* and *b* and the reflectance of the episcotister, *r*.

$$p = ta + (1 - t)r \tag{1}$$

$$q = tb + (1 - t)r \tag{2}$$

By solving these equations, the two unknowns *t* and *r* can be described as follows:

$$t = \frac{p - q}{a - b} \tag{3}$$

$$r = \frac{aq - bp}{a - b - p + q} \tag{4}$$

This original episcotister model has been modulated by Gerbino (Gerbino, 1994; Gerbino, Stultiens, Troost, & de Weert, 1990) to express more general situations. Gerbino used luminance instead of reflectance as the independent variable and reformulated the equations so that the model can be used for the condition in which two overlapping surfaces are differently illuminated. In Gerbino's model, they explicitly assumed a physical configuration in which a transparent surface is overlaid on an opaque surface (Figure 2B), and the luminance of the two regions *p* and *q* in the transparent surface is described as follows:

$$p = ta + F \tag{5}$$

$$q = tb + F \tag{6}$$

where *a* and *b* represent the luminance of the two corresponding regions in the background surface (see Figure 2C), *t* is the transmittance of the transparent surface, and *F* represents the luminance reflected from the transparent surface. By solving these equations, the two unknowns *t* and *F* can be described as follows:

$$t = \frac{p - q}{a - b} \tag{7}$$

$$F = \frac{aq - bp}{a - b} \tag{8}$$

Kitaoka (2005) demonstrated that the constraints derived from these equations are consistent with the categorization given by the Adelson-Anandan-Anderson contrast polarity rule. Given a configuration like Figure 1, there are in general four possible interpretations if we consider that there is a transparent surface comprising two adjacent regions. Those possible transparent surfaces are *pq*, *bq*, *ap*, and *ab*. (Here, we ignore the effect from the figural constraints.) It is known that there is another possible interpretation in which a surface is partially transparent and partially opaque, which is known as partial transparency (Beck et al., 1984; Metelli, 1974a; Metelli, Da Pos, & Cavedon, 1985). It is also possible that a transparent surface comprising two regions with different surface properties is fully covering the other opaque surface, which is known as full-layer transparency (Kitaoka, 2005). Here, for brevity, we consider only the first four interpretations mentioned; these four are the most parsimonious interpretations. For each of the four interpretations, the transmittance t and the reflected luminance F of the transparent surface can be written using luminance a, b, p, and q as in Equations 7 and 8 in the case that *pq* is assumed to be the transparent surface. From these equations, we can obtain three rules that must be satisfied for each interpretation to be physically valid under the assumptions that transmittance is modeled by a proper fraction (i.e., a number between zero and one) and reflected luminance is a natural quantity (i.e., a nonnegative physical value). For example, under the interpretation that *pq* is the transparent surface, the three rules can be described as follows:

(1) If $a > b$, then $p > q$; if $a < b$, then $p < q$ ($\because t > 0$).
(2) $|a - b| \geq |p - q|$ ($\because t \leq 1$).
(3) If $a > b$, then $aq \geq bp$; if $a < b$, then $aq \leq bp$ ($\because F \geq 0$).

Rule 1 is obtained from the physical constraint that the transmittance t in Equation 7 should be larger than zero. This rule formulates the constraint regarding the invariance of contrast polarity along the pair of aligned "background" contours p/q and a/b, which is preserved in single-reversing (Figure 1A) and nonreversing (Figure 1B) X-junctions, according to the categorization of X-junctions by the Adelson-Anandan-Anderson contrast polarity rule. Rule 2 is obtained from the constraint that the transmittance t in Equation 7 should not be larger than one. Finally, rule 3 is obtained from the constraint that the luminance reflected from the transparent surface (i.e., F in Equation 8) should not be less than zero. First, let's consider the single-reversing junction in Figure 1A. In this case, all three rules are satisfied under the interpretation that *pq* is the transparent surface. Rule 1 is not satisfied under the interpretation that *bq* is the transparent surface. Rules 1 and 3 are not satisfied under the interpretation that *ap* is the transparent surface. Rules 2 and 3 are not satisfied under the interpretation that *ab* is the transparent surface. Therefore, the reason why the surface *pq* is always perceived as being in front in Figure 1A can be because it is the only solution that is a physically valid interpretation. Second, as for the double-reversing junction (Figure 1C), rule 1 is not satisfied under any of the four interpretations. In this case, any transparency perception is denied because any interpretation is physically invalid. Finally, as for the nonreversing junction (Figure 1B), rule 1 is always satisfied under any of the four interpretations while the other rules are either satisfied or not depending on the actual luminance values of each region. For example, given a nonreversing junction pattern that has the luminance combination $(a, b, p, q) = (90, 30, 50, 20)$, the properties of possible transparent surfaces (t, F) are (0.5, 5) for the surface *pq*, (0.25, 7.5) for the surface *bq*, (4, −30) for the surface *ap*, and (2, −10) for the surface *ab*. In this case, all four interpretations satisfy rule 1 since $t > 0$ for every interpretation. However, rules 2 and 3 are violated under the surface *ap* and surface *ab* interpretations since $t > 1$ and $F < 0$, whereas they are satisfied under the surface *pq* and surface *bq* interpretations since $t \leq 1$ and $F \geq 0$. Thus, for this pattern, the two interpretations are physically valid but the others are not. On the other hand, if the luminance combination (a, b, p, q) is (90, 40, 30, 10), the properties of possible transparent surfaces (t, F) are (0.4, −6) for the surface *pq*, (0.5, −5) for the surface *bq*, (2, 10) for the surface *ap*, and (2.5, 15) for the surface *ab*. In this case, rule 1 is always satisfied but either rule 2 or rule 3 is violated under every interpretation, which means that every interpretation is physically invalid under this condition. Likewise, for every possible nonreversing junction pattern, the physical photometric model does not provide a unique solution in which only one interpretation is physically valid; sometimes there are two valid interpretations and sometimes there are none. This could be the reason why the interpretation of nonreversing junctions is considered ambiguous or indeterminate.

Perceived depth ordering in bistable transparency

The Adelson-Anandan-Anderson contrast polarity rule characterizes the bistable transparency patterns as those that leave ambiguity in perceived depth ordering;

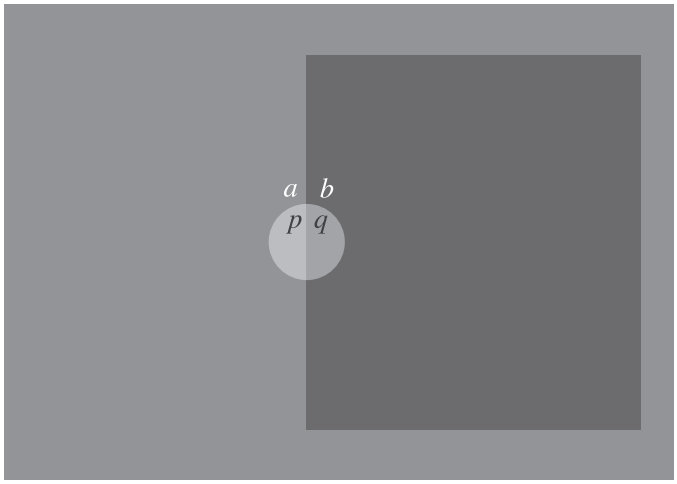

Figure 3. An example of the stimuli used in the experiment by Delogu et al. (2010).

this can be explained by considering the physical photometric constraints as described in the previous section. However, previous studies have found that the visual system still shows preferences for a specific interpretation of depth ordering when viewing bistable transparency patterns (Beck et al., 1984; Delogu et al., 2010; Kitaoka, 2005; Oyama & Nakahara, 1960). Delogu et al. (2010) argued that an additional photometric rule, the transmittance anchoring principle (TAP) proposed by Anderson (2003), might explain this behavior. The TAP argues that "the highest contrast region along a continuous contour that undergoes changes in contrast magnitude, while preserving contrast polarity, will appear as a surface in plain view, whereas lower values of contrast along such contours are decomposed into multiple layers" (Anderson, 2003, p. 795). Taking into account this notion, Delogu et al. (2010) proposed a model that can explain perceived depth ordering of bistable transparency patterns examined in their experiment. In their study they used patterns in which two objects defined by closed contours (one is a disk and the other is a rectangle) are partially overlapping with each other (Figure 3). In this case, perceived interpretations can often be restricted to two alternatives ("the disk pq is in front of the rectangle bq" or "the rectangle bq is in front of the disk pq") due to the figural constraints. Thus, their model was designed to predict the likelihood of the occurrence of these two alternatives. One can describe the prediction by their model as follows:

(i) If $|p-q|+|p-a|<|b-q|+|b-a|$, the disk pq is perceived as being in front.
(ii) If $|p-q|+|p-a|>|b-q|+|b-a|$, the rectangle bq is perceived as being in front where a, b, p, and q represent lightness of the corresponding regions.

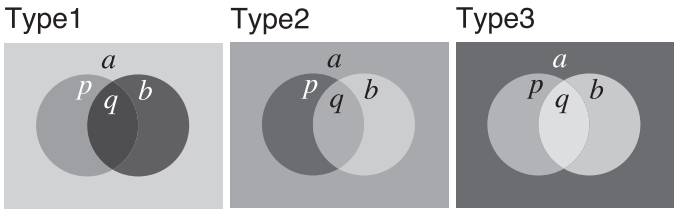

Figure 4. Three types of bistable transparency patterns. Bistable transparency patterns can be classified into three categories based on the contrast polarity along the edges of each region.

To translate luminance into lightness, they used an equation proposed by Wyszecki (1963), which is

$$W = 25Y^{1/3} - 17, \quad (9)$$

where W is the lightness value and Y is the luminance level. Here, the smaller $|p-q|$ is and the larger $|b-a|$ is, the more likely rule 2 is satisfied under the assumption that the surface pq is in front. The smaller $|p-a|$ is and the larger $|b-q|$ is, the less likely rule 2 is satisfied under the assumption that the surface bq is in front. Thus, their model is consistent with the physical photometric model except that it depends on lightness, not luminance. They assumed that the ambiguity in perceived depth ordering arises only when both regions p and b have the same lightness difference with all flanking regions. In those cases, they found that the surface including the region showing the smaller difference in lightness with the region q is more likely to be perceived as being in front. They modeled this tendency as follows:

(iii) If $|p-q|+|p-a|=|b-q|+|b-a|$, the preferences for "disk in front" perception follows a value $|b-q|-|p-q|$.

Thus, their model can be divided into two stages. In the first stage, which corresponds to i and ii in the above description, the visual system determines depth ordering in a way that is moderately consistent with the physical photometric rules. If the comparison falls on the decision criterion, the decision is suspended until the second stage. The ambiguity arises only at this stage.

Nevertheless, it still remains unclear whether their model can be applied to any luminance combinations in bistable transparency. One reason is that they estimated their model using stimuli within largely restricted dimensional space. For example, given a bistable transparency pattern comprising two objects, there are actually three possible situations when classification is based on the contrast polarity along the edges of each region (Figure 4). In the study by Delogu et al. (2010), they tested only about 20 patterns of Type 2 in Figure 4, keeping the luminance of the background region constant.

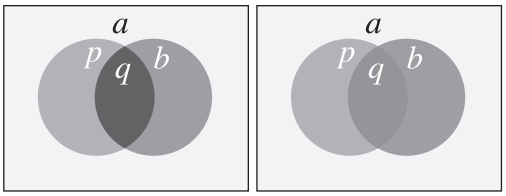

Figure 5. An example of the stimulus pair for which the model by Delogu et al. (2010) cannot explain the difference in percentage "left in front." The difference in the two images exists only in lightness of the region q. Thus, $|b-q|-|p-q|$ of the left image is the same as that of the right image. However, the left disk appears to be in front more often in the left image than in the right image (percentage "left in front" examined in our experiment was 49% for the left image and 22% for the right image).

Moreover, in their study, at least one of the two alternative interpretations (disk in front or rectangle in front) was always consistent with rule 2 of the photometric constraint. Therefore, it is not clear what happens if both of the two alternatives favored by the figural constraint do not satisfy the photometric constraint. Several previous studies have shown that the visual system often adopts interpretations that violate the photometric constraint, especially when there is a strong figural constraint (Beck & Ivry, 1988; Beck et al., 1984; Kitaoka, 2005). Investigating the perceived depth ordering under such conditions might help clarify a photometric factor that is independent of the physical photometric constraint.

Finally, in their model, the preferences for "disk in front" perception were modeled as being proportional to the subtractive difference between two lightness differences (i.e., $|b-q|-|p-q|$). Although this could be the simplest formulation to represent a difference between two contrasts, it is not appropriate when modeling the perceived size of the difference. The visual system tends to overestimate the difference when the absolute levels of the contrasts are small and underestimate the difference when they are large. We think that this nonlinearity in subjective contrast difference should be incorporated into the model of the perceived depth ordering. In Figure 5, we show an example in which this is the case. In this figure, each corresponding region in the two Type 1 stimuli has the same luminance except for the region q, and we expect that most of the people seeing them would feel that the left disk (the surface pq) appears to be in front more often in the left image than it does in the right image. Here we demonstrate that the model by Delogu et al. (2010) cannot explain this tendency. In the first stage of their model, the sum of the lightness differences $|p-q|+|p-a|$ is compared with the other sum of the lightness differences $|b-q|+|b-a|$. In this example, $|p-q|+|p-a|$ is exactly the same as $|b-q|+|b-a|$ for both images. (In fact, any of the Type 1 and Type 3 stimuli always satisfies $|p-q|+|p-a|=|b-q|+|b-a|$.) In this case, the analysis proceeds to the second stage, and the likelihood of occurrence of "left disk in front" interpretation is determined as being proportional to $|b-q|-|p-q|$. However, $|b-q|-|p-q|$ equals $b-p$ whenever a pattern belongs to Type 1 stimuli. Therefore, the difference in the likelihood of occurrence of specific perceived depth ordering seen in Figure 5 is not explained by the model by Delogu et al. (2010). (Likewise, $|b-q|-|p-q|$ equals $p-b$ whenever a pattern belongs to Type 3 stimuli, and the same deviation from their model would occur in the case of Type 3 stimuli.) Nevertheless, if we consider that the perceived depth ordering is determined not by the simple subtractive difference between $|b-q|$ and $|p-q|$ but by the subjective difference between them such as defined in Equation 10, we would be able to easily explain the tendency observed in Figure 5.

$$\rho=\frac{|b-q|-|p-q|}{|b-q|+|p-q|} \tag{10}$$

The present study was aimed at investigating if the model defined in Equation 10 can better explain the perceived depth ordering. In our experiment, we used a larger number of bistable transparency patterns (562 patterns in total). The patterns comprised two moving objects defined by closed contours and included all stimulus types defined in Figure 4. Thus, our study was also focused on investigating the perceived depth ordering under the condition in which possible transparent surfaces can be restricted to two alternatives (i.e., "left disk in front" or "right disk in front") by the figural constraints. In a portion of those stimuli, both of those alternatives were consistent with the physical photometric constraint. In the other stimuli, either or both of those alternatives were inconsistent with rules 2 or 3 of the photometric constraint. As a result of the experiment, we found that the model defined in Equation 10, calculated based on lightness, can explain the perceived depth ordering of those stimuli irrespective of the stimulus types and independent of whether the figural constraints were consistent with the photometric constraint.

Methods

Subjects

Twelve subjects (aged 22–42) who were unaware of the purpose of the experiment participated in the study. All subjects had normal or corrected-to-normal visual acuity. The experiment in this study was conducted in accordance with the Declaration of Helsinki.

Apparatus

Stimuli were presented in a dark room on a CRT monitor (Trinitron Multiscan CPD-17SF9, Sony, Tokyo, Japan; 17 in., 1024 × 768 pixels, refresh rate 75 Hz, mean luminance 44.6 cd/m^2). Each subject placed his or her head on a chin rest and used both eyes to view the stimuli. The viewing distance was 86 cm.

Stimuli

To prevent the effect of size information that could influence depth-order perception (Delogu et al., 2010), we used stimuli that had symmetric shapes (Figure 4). A stimulus comprised two disks of the same size (diameter was 5.1°). In the presentation we made the stimulus move horizontally in a symmetrical fashion because a previous study suggested that motion can reduce inconsistency in depth-order perception without distorting the mean response (Experiment 1 in Delogu et al., 2010). For each presentation, the two disks first appeared at both sides of the screen. Immediately after the onset of the disks, the disks started moving horizontally toward the center of the screen. The movement of the disks was sinusoidally modulated and the disks reversed their direction of motion when their center locations reached 0.63° away from the screen center (for details, see Figure 6). The disks disappeared when they returned to their initial onset locations. Thus, when the two disks were overlapping, the whole image of the stimuli had four regions: background region (*a*), right disk region (*b*), left disk region (*p*), and shared region (*q*). All of the *a*-*b*-*p*-*q* combinations of luminance values tested in this study are shown in Table 5 in Appendix B. Of the 562 stimuli, 180 stimuli belonged to Type 1, 208 stimuli belonged to Type 2, and 174 stimuli belonged to Type 3 of the bistable transparency pattern. We generated the stimulus patterns so that each luminance of the regions *a*, *b*, *p*, and *q* was independently and uniformly modulated in lightness domain as defined in Equation 9.

Procedure

In each trial the dynamic stimulus, comprising the two disks, was presented for 1.3 s (as shown in Figure 6). After that a blank with a fixation point followed, during which time the observer performed a task of judging by button press whether the left disk appeared behind or in front of the right disk. However, the possible perceptual patterns were not restricted to those two alternatives. For example, the whole surface with a hole shaping a disk might be perceived as being in front. In this case and other such cases, the observer

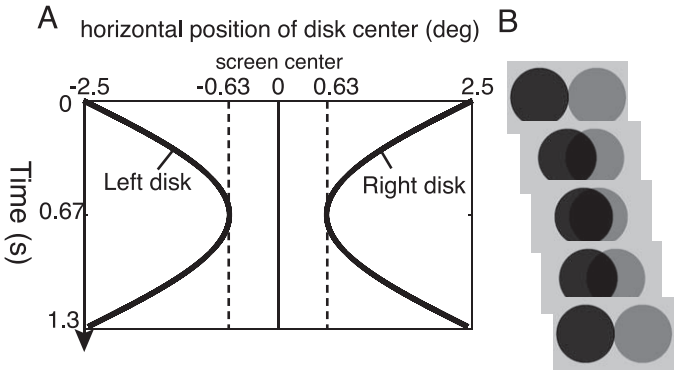

Figure 6. Time course of the stimulus presentation. (A) The spatiotemporal plot of the movement of the disks. The black curves indicate the horizontal position of the center of the two disks relative to the screen center. (B) Snapshots of the actual display at several times on the spatiotemporal plot.

was told to cancel that trial by pressing the third button. The observer could also cancel any trial if she or he could not reasonably understand the structure of the stimulus. The next trial started immediately after the observer pressed a key. The fixation point was presented at the center of the screen at the beginning of each session and during every blank period. To minimize the effect of adaptation to the background intensity in the previous trial, the background intensity during the blank period was set to that of the background region (*a*) of the next trial's stimulus, except for the last trial in each session, in which the background intensity during the blank period was the same as that of the preceding stimulus.

In one session, 281 stimuli were randomly chosen from all of the 562 stimuli and tested in a random order. The remaining 281 stimuli were tested in the next session. Twelve observers completed six sessions. Therefore, 36 responses were collected for each stimulus.

Results

We calculated the probability that the left disk was perceived as being in front of the right disk for each stimulus from the responses in the trials that the subjects did not cancel. The percentage of "left in front" and the percentage of the canceled trials for each stimulus are shown in Table 5 in Appendix B. The percentage of canceled trials in all the responses for each stimulus was 2.8% on average and 22.2% at most. Because enough responses for calculating percentage "left in front" were obtained for every stimulus, we used the data from all the stimuli in the following analysis.

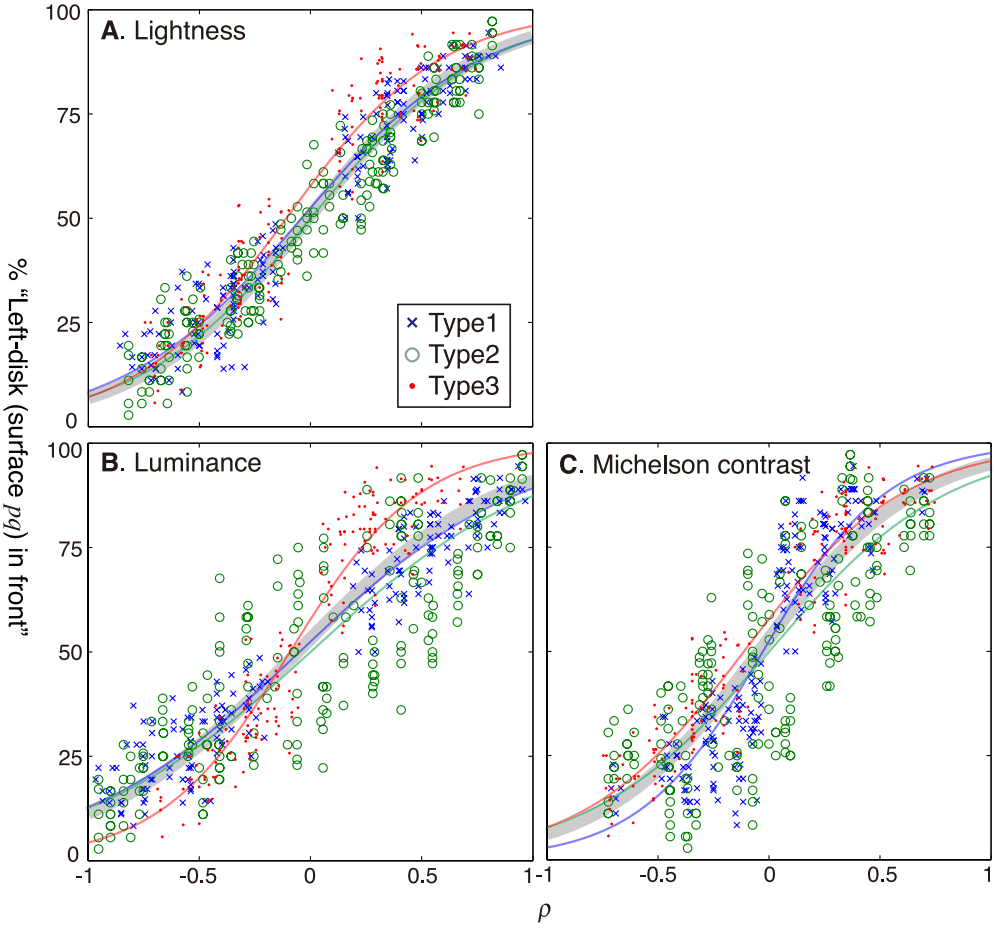

Figure 7. Percentage "left in front" plotted as a function of the relative contrast ratio ρ (Equation 10). The thick gray curve shows the best-fit sigmoid function (Equation 12) for the entire data set. The red, green, and blue curves show the best-fit sigmoid functions for the data of Type 1, Type 2, and Type 3 stimuli, respectively. In (A), ρ was calculated based on lightness; in (B), ρ was calculated based on luminance; and in (C), ρ was calculated based on Michelson contrast.

Relative contrast difference against shared region q is the major determinant of depth-order preferences in bistable transparency

First, we examined how much the model defined in Equation 10 can explain the data of percentage "left in front." Here, we expected that lightness difference, not luminance difference, should be used as the contrast between the two abutting regions. Although Delogu et al. (2010) used the cube-root formula in Wyszecki (1963) to calculate lightness value from luminance level, what exponent best predicts the depth-order perception observed in our study should also be an empirical matter. In the present study, therefore, we let the translation exponent be a free parameter and estimated the best one. The equation used to translate luminance into lightness was as follows:

$$l' = l^n \tag{11}$$

where l represents normalized luminance level (luminance divided by the maximum luminance 89.2 cd/m^2) and l' represents lightness value. Thus, we substituted the lightness values obtained by this equation into Equation 10 and plotted each percentage "left in front" as a function of ρ (Figure 7A). In order to estimate the best exponent as well as to establish a quantitative measure of goodness of prediction of the model, we fitted a sigmoid function (Equation 12) to the data in logistic regression.

$$y = \frac{100}{1 + e^{-\frac{x-m}{s}}} \tag{12}$$

The thick gray curve in Figure 7A shows the best-fit sigmoid function for the entire data set including all of the stimulus types. The best-fit parameters of the sigmoid function and the coefficient of determination (R^2) are shown in Table 1. The exponent obtained by the fitting analysis was 0.46. This is relatively larger than that in the cube-root formula (such as in Equation 9 or Munsell's formulation) but very close to the square-root exponent that was used to explain perceived lightness in some previous studies (Warren &

Metric to calculate contrast	Stimulus type	Best-fit parameters	R^2
Lightness (Figure 10A)	All	n = 0.46, m = −0.01, s = 0.38	0.88
	Type 1	m = −0.04, s = 0.40	0.91
	Type 2	m = 0.00, s = 0.39	0.90
	Type 3	m = −0.11, s = 0.35	0.89
Luminance (Figure 10B)	All	m = −0.06, s = 0.46	0.78
	Type 1	m = −0.05, s = 0.50	0.91
	Type 2	m = 0.00, s = 0.52	0.72
	Type 3	m = −0.09, s = 0.29	0.87
Michelson contrast (Figure 10C)	All	m = −0.04, s = 0.35	0.71
	Type 1	m = −0.03, s = 0.28	0.76
	Type 2	m = 0.00, s = 0.40	0.58
	Type 3	m = −0.11, s = 0.36	0.89

Table 1. The results of the fitting analysis for the data plotted based on ρ (Figure 10). The sigmoid function (Equation 12) was fitted to the entire data set as well as to the data of each stimulus type. For the case of lightness contrast, the translation exponent n in Equation 11 was also searched for in the fitting analysis for the entire data set. The best-fit parameters are shown in the third column. The coefficients of determination (R^2s) are shown in the fourth column.

Poulton, 1960, 1966). Using the best-fit exponent $n = 0.46$, we also fitted different sigmoid functions to different stimulus type data separately. The best-fit parameters of these sigmoid functions and the coefficients of determination (R^2s) are also shown in Table 1.

Since the kind of representation the transparency perception is based on is one of the important issues (Anderson, Singh, & Meng, 2006; Singh & Anderson, 2002), we also tested other metrics (i.e., luminance difference and Michelson contrast) to calculate contrast (difference) between two regions. In Figure 7, we plotted percentage "left in front" as a function of ρ (Equation 10) calculated according to each metric of contrast (Figure 7B for luminance difference, Figure 7C for Michelson contrast). For the case of luminance difference, we substituted the luminance level directly into Equation 10 to obtain ρ. For the case of Michelson contrast, we substituted the luminance level of each region a, b, p, and q into the following equation to obtain ρ:

$$\rho = \left(\frac{|b-q|}{b+q} - \frac{|p-q|}{p+q}\right) \Big/ \left(\frac{|b-q|}{b+q} + \frac{|p-q|}{p+q}\right) \quad (13)$$

Again, we fitted a sigmoid function to the entire data set including all of the stimulus types (gray curves) and to the data of each stimulus type (blue, red, and green curves for Type 1, Type 2, and Type 3, respectively). The best-fit parameters and the coefficient of determination (R^2) of each fitting are shown in Table 1. As shown in R^2 in Table 1, the model fit to the entire data set was better when we used lightness difference ($R^2 = 0.88$) than when we used luminance difference ($R^2 = 0.78$) and Michelson contrast ($R^2 = 0.71$), which indicated that lightness difference was the most reliable metric among the three to predict the depth-order perceptions observed in our experiment.

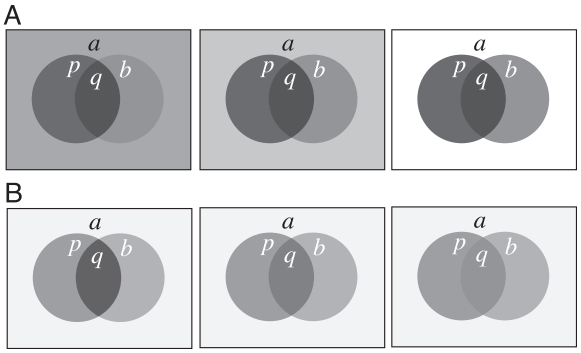

Figure 8. The comparison between the effect of the background region *a* and that of the shared region *q*. (A) Percentage "left in front" did not change much when only the intensity of the background *a* was varied. (B) Percentage "left in front" changed according to the proposed model ρ (Equation 10) when only the intensity of the shared region *q* was varied. For both cases, percentage "left in front" should increase from the left image to the right image if the visual system prefers the surface with smaller physical transmittance.

The high predictability by the model ρ (Equation 10) suggested that taking into account the contrast against the background region a (i.e., $|b-a|$ and $|p-a|$) was not relevant to predicting depth-order perception in bistable transparency patterns. To further clarify this point, we conducted another statistical analysis. In this analysis, we extracted groups of the stimuli such that only luminance of the background region a was varied within each group and tested whether percentage "left in front" was changed within each group. An example of this is shown in Figure 8A. According to the previous models such as that by Delogu et al. (2010) and the TAP, a possible effect of the background region is that percentage "left (surface pq) in front" increases as contrast between b and a increases with respect to contrast between p and a. Thus, we plotted percentage "left in front" based on $(|b-a| - |p-a|)/(|b-a| + |p-a|)$ and fitted a sigmoid function for the data within each group. Here we consistently used $n = 0.46$ to calculate lightness value using Equation 11. Then, we examined whether the average of the slopes (i.e., $1/s$) of the sigmoid functions was significantly larger than zero. By this within-group analysis, we could isolate the effect of the background region a from that of the region q. The average of the best-fit slopes ($1/s$) was 0.06 for Type 1 stimuli, 0.10 for Type 2 stimuli, and 1.24 for Type 3 stimuli. Single-sample t-tests revealed that the averaged slope was significantly larger than zero only for Type 3 stimuli [$t(43) = 2.52$, $p = 0.02$]; it

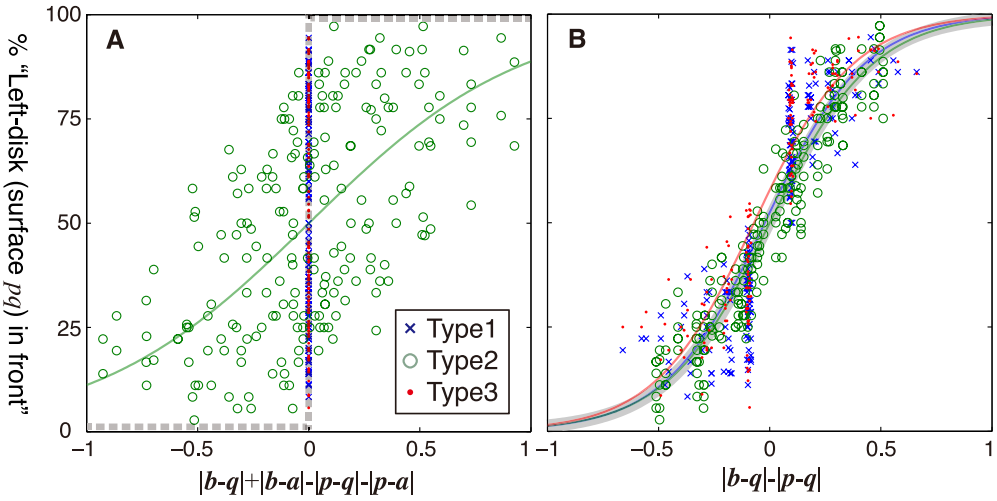

Figure 9. The data plotted according to the model proposed by Delogu et al. (2010). (A) The data plotted based on $|b-q|+|b-a|-|p-q|-|p-a|$. If the data obtained in our experiment followed the model by Delogu et al. (2010), percentage "left in front" should be nearly zero in the left side of the plot and nearly 100% in the right side of the plot (as represented by the gray broken curve). The green curve shows the best-fit sigmoid function (Equation 12) for the data of Type 2 stimuli. (B) The data plotted based on $|b-q|-|p-q|$. According to the model by Delogu et al. (2010), if $|p-q|+|p-a|$ is similar to $|b-q|+|b-a|$, percentage "left in front" should be proportional to a value $|b-q|-|p-q|$. The thick gray curve shows the best-fit sigmoid function for the entire data set. The red, green, and blue curves show the best-fit sigmoid functions for the data of Type 1, Type 2, and Type 3 stimuli, respectively.

was not significant for Type 1 stimuli [$t(43)=0.14$, $p=0.88$] or for Type 2 stimuli [$t(47)=1.38$, $p=0.17$]. For comparison, we also extracted groups of stimuli where only luminance of the overlapping region q was varied (see Figure 8B) and conducted the same analysis; namely, we plotted percentage "left in front" based on $(|b-q|-|p-q|)/(|b-q|+|p-q|)$ and fitted a sigmoid function for data within each group. The average of the best-fit slopes ($1/s$) was 2.25 for Type 1 stimuli, 2.50 for Type 2 stimuli, and 2.33 for Type 3 stimuli. Single-sample t-tests revealed that the averaged slope was significantly larger than zero for all stimulus types [$t(33)=4.89$, $p<0.001$ for Type 1 stimuli; $t(47)=30.95$, $p<0.001$ for Type 2 stimuli; and $t(35)=5.56$, $p<0.001$ for Type 3 stimuli]. Thus, the effect of the background region in depth-order perception was negligible for most of the cases except Type 3 stimuli. Conversely, the contrast against the shared region was the major determinant for depth-order perception in bistable transparency patterns.

Finally, as a comparison, we tested how much the model proposed by Delogu et al. (2010) can explain our data. The model by Delogu et al. (2010) predicts the perceived depth ordering as follows:

(i) If $|p-q|+|p-a|<|b-q|+|b-a|$, the left disk pq is perceived as being in front,
(ii) if $|p-q|+|p-a|>|b-q|+|b-a|$, the right disk bq is perceived as being in front, and
(iii) if $|p-q|+|p-a|=|b-q|+|b-a|$, percentage "left in front" follows a value $|b-q|-|p-q|$,

where a, b, p, and q represent lightness of the corresponding regions. We first tested i and ii of their model. In Figure 9A, we plotted percentage "left (surface pq) in front" based on $|b-q|+|b-a|-|p-q|-|p-a|$ and fitted a sigmoid function to the data. To make the comparison fair, we used Equation 11 to

Model	Stimulus type	Best-fit parameters	R^2
$\|b-q\|+\|b-a\|-\|p-q\|-\|p-a\|$ (Figure 9A)	Type 2	n = 0.49, m = −0.00, s = 0.48	0.35
$\|b-q\|-\|p-q\|$ (Figure 9B)	All	n = 0.43, m = −0.01, s = 0.23	0.75
	Type 1	m = −0.02, s = 0.22	0.72
	Type 2	m = 0.00, s = 0.23	0.86
	Type 3	m = −0.07, s = 0.22	0.69

Table 2. The results of the fitting analysis for the data plotted based on the model by Delogu et al. (2010). The sigmoid function (Equation 12) was fitted to the data of Type 2 in Figure 9A and was fitted to the entire data set as well as to the data of each stimulus type in Figure 9B. The translation exponent n in Equation 11 was also searched for in the fitting analysis in Figure 9A and in the fitting analysis for the entire data set in Figure 9B. The best-fit parameters are shown in the third column. The coefficients of determination (R^2s) are shown in the fourth column.

calculate lightness and estimated the best exponent n for this plot. Because Type 1 and Type 3 stimuli always satisfy $|b-q|+|b-a|-|p-q|-|p-a|=0$ irrespective of the translation exponent n, the fitting analysis was conducted only for the data of Type 2 stimuli. The green curve in Figure 9A shows the best-fit sigmoid function. The best-fit exponent was 0.49. The best-fit parameters and the coefficient of determination (R^2) are shown in Table 2. If the data obtained in our experiment followed the model by Delogu et al. (2010), percentage "left in front" should be nearly zero in the left side of the plot in Figure 9A and nearly 100% in the right side of the plot. Ambiguity should remain around the origin of the abscissa. This prediction is represented by the gray broken curve in Figure 9A. However, the actual data of Type 2 stimuli show substantial variation in almost every region of the plot. The coefficient of determination (R^2) obtained by the fitting analysis for the data also shows much deterioration compared with that obtained with the model ρ defined in Equation 10. Since the variation that was not predicted by the first stage could be explained by the second stage of their model, we then plotted all the data based on $|b-a|-|p-q|$ in Figure 9B. Again, we fitted a sigmoid function to the entire data set and obtained the best-fit exponent $n=0.43$. The thick gray curve in Figure 9B shows the best-fit sigmoid function. The best-fit parameters and the coefficients of determination (R^2) are shown in Table 2. To see if there was any difference between different stimulus types, we also fitted a sigmoid function to the data of each stimulus type separately using the exponent $n=0.43$. The best-fit parameters and the coefficients of determination (R^2) are shown in Table 2. As shown in Figure 9B and by R^2 in Table 2, the prediction by the second stage of the model by Delogu et al. (2010) was better than that by the first stage. Nevertheless, it was still worse compared with the prediction by ρ in Equation 10. Every coefficient of determination (R^2) obtained by using the model by Delogu et al. (2010) was lower than those obtained by using the model ρ.

The relationships between the physical photometric constraint and the perceived depth ordering

In the previous section, we showed that relative size of the lightness difference against the shared region q was the most important photometric factor to explain the perceived depth ordering. The lightness difference against background region a had little influence. This suggested that the visual system relies on its own criterion, which is independent of the physical photometric constraint, because the physical photometric constraint involves not only contrast against the region q but also contrast against the region a (see rules 1 through 3 in "Classification of perceptual transparency based on Adelson-Anandan-Anderson's contrast polarity rule"). However, in the previous section, we did not classify the data according to the physical photometric condition. Thus, some difference might be found if we analyzed the data separately, considering the conditions in which the figural constraints were consistent with the photometric constraint and those conditions in which they were not consistent. To clarify this point, we classified all the stimuli based on which interpretation the photometric constraint supports. Let us take for example a stimulus that has a combination of normalized luminance (a, b, p, q) = (89.8, 35.3, 9, 4.7). In this case, the transmittance t and reflected luminance F of possible transparent surfaces are (t, F) = (0.0789, 1.91) for the surface pq, (0.379, 1.29) for the surface bq, (2.64, −3.41) for the surface ap, and (12.7, −24.3) for the surface ab. Thus, this stimulus is classified into a group where both the "surface pq in front" interpretation and the "surface bq in front" interpretation are valid (pq and bq valid group) because rules 2 ($t \leq 1$) and 3 ($F \geq 0$) are satisfied under those interpretations while they are violated under the other interpretations. There were five groups in total: "pq and bq valid," "pq and ap valid," "bq and ab valid," "ap and ab valid," and "all invalid." When either rule 2 or 3 was violated under all four interpretations (i.e., pq in front, bq in front, ap in front, and ab in front), the stimulus was classified as "all invalid." In Appendix A, we show a brief summary of each of those groups.

In our experiment, the figural constraints (i.e., the closed contours and their motion) strongly indicated that the disks (the surface pq and the surface bq) are figural objects. Therefore, if we investigated the data in the "pq and bq valid" group, we might be able to find some dependency on the physical photometric constraint, excluding the effect of the figural constraints. First, we separately plotted the data in each group based on ρ in Equation 10 (Figure 10A-1, A-2). We used the exponent $n=0.46$ in translating luminance into lightness. In Figure 10A, the data of each group are plotted in different colors and symbols. The curves indicate the best-fit sigmoid function for the data with the same color. The best-fit parameters and the coefficients of determination (R^2s) are shown in Table 3. The curves were quite similar with each other, and all data were reasonably explained by Equation 10 irrespective of the physical photometric conditions.

To further show that the data were independent of the physical filter property, we also tested if the model that explicitly incorporated the transmittance t of the surface pq and the surface bq can explain the data. According to rule 2 of the physical photometric constraint, a possible strategy is to choose a surface with smaller transmittance as a filter for being in front.

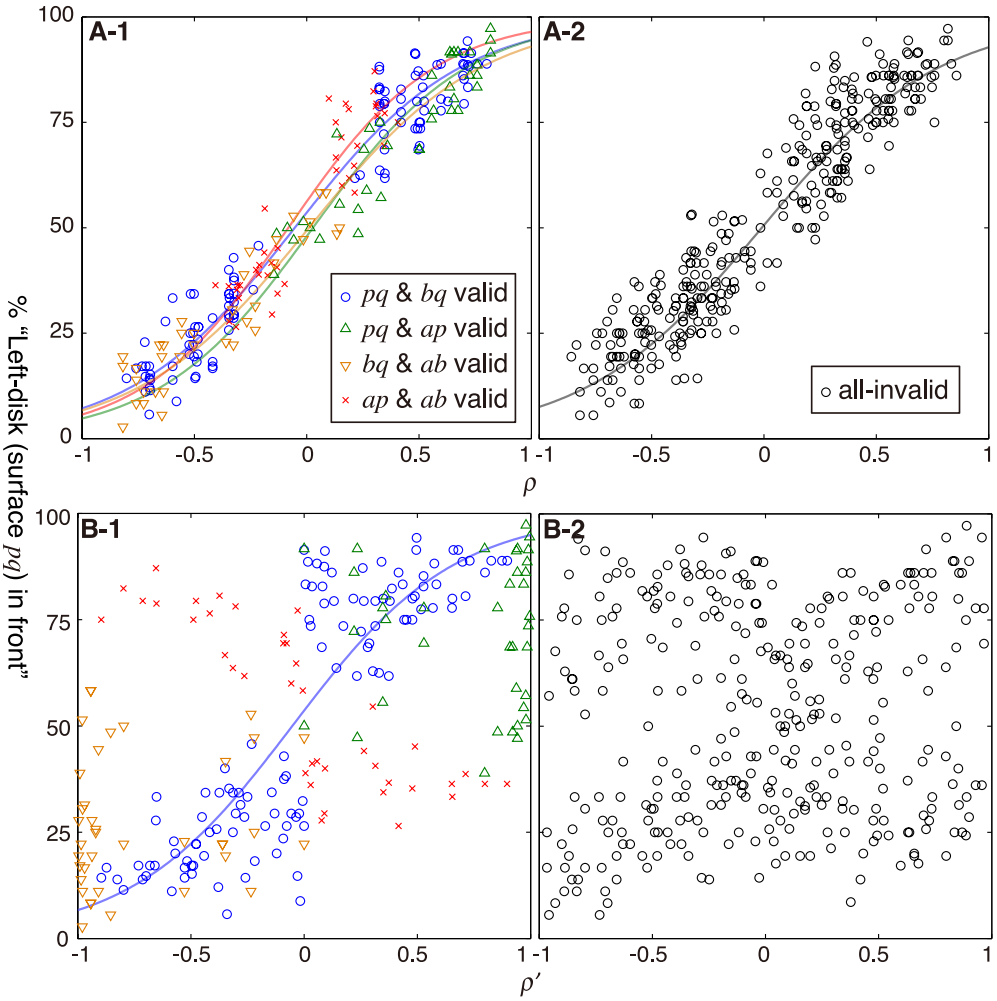

Figure 10. (A) Percentage "left in front" plotted based on ρ (Equation 10). The model reasonably predicted the results irrespective of the physical photometric condition. The data that belong to different groups are distinguished by different colors and symbols. The curves indicate the best-fit sigmoid function for the data with the same color. (B) Percentage "left in front" plotted based on ρ' (Equation 14), in which the physical transmittance is incorporated to explain the data. The blue curve in B-1 indicates the best-fit sigmoid function for the data of the "*pq* and *bq* valid" group.

Although there are several ways to formulate such a strategy, we used the following equation since it was simple and comparable with the proposed model ρ (Equation 10).

$$\rho' = \frac{t_{bq} - t_{pq}}{t_{bq} + t_{pq}} \tag{14}$$

where t_{bq} and t_{pq} are the transmittance of the surface *bq* $(b - q/a - p)$ and the surface *pq* $(p - q/a - b)$, respectively. In Figure 10B (B-1, B-2), we plotted the data of each group based on this equation. We also tried to fit a sigmoid function to the data of each group, but we could obtain a reasonable function only for the data of the "*pq* and *bq* valid" group. The best-fit parameters

	ρ (Equation 10)		ρ' (Equation 14)	
Group	Best-fit parameters	R^2	Best-fit parameters	R^2
pq and *bq* valid	m = −0.05, s = 0.37	0.93	m = −0.05, s = 0.36	0.73
pq and *ap* valid	m = 0.03, s = 0.34	0.79	–	–
bq and *ab* valid	m = 0.01, s = 0.38	0.76	–	–
ap and *ab* valid	m = −0.08, s = 0.33	0.83	–	–
All invalid	m = −0.01, s = 0.40	0.86	–	–

Table 3. The best-fit parameters of the sigmoid functions in Figure 10 and their coefficients of determination, R^2. A dash (–) indicates that the best-fit parameters or the coefficient of determination were not available in that group.

and the coefficient of determination (R^2) are shown in Table 3. For the other groups, the model ρ' did not make any good prediction at all. This is thought to be a natural consequence given that there is no reason that the visual system has to represent ecologically invalid transmittance values. Comparing transmittance values would be possible only when both transmittances were less than one, like in the case of the "*pq* and *bq* valid" condition. However, it should be noted that even in the "*pq* and *bq* valid" condition, the goodness of prediction by ρ' was worse than that by ρ in Equation 10. We also tested if other models, which incorporated reflected luminance F too (e.g., a model in which more reflected surface is likely perceived as being in front), would be able to explain the data in several formulations, but could not find any model that explained the data better than the proposed model ρ. Therefore, given that the simpler model ρ could explain the data consistently, irrespective of the physical photometric conditions, it would be the most parsimonious conclusion that the visual system uses this criterion without explicitly considering the physical filter property.

Discussion

Contrast against a shared region is the major determinant for perceived depth ordering in bistable transparency

In this study, we presented bistable transparency patterns in which two horizontally moving disks appeared to partially overlap with each other and obtained percentage "left in front" for 562 test patterns. From the data, we investigated what the major determinant for perceived depth ordering in bistable transparency is. The previous study that used similar test patterns argued that contrast against the shared region and contrast against the background region equally contribute to depth-order perception for bistable transparency patterns unless both surfaces are equally contrasted against all surrounding regions (Delogu et al., 2010). However, the present study demonstrated that contrast against the background region has little influence on depth-order perception as compared with the influence of contrast against the shared region. In addition, we found that the relative contrast difference ρ (Equation 10), instead of the simple subtractive difference, can provide a better prediction for perceived depth ordering. In the discussion of experiment 2 in the study by Delogu et al. (2010), they argued that the contrast against the overlapping region alone could not entirely explain the results because they found a significant difference in the depth-order perceptions between a stimulus pair whose lightness configurations were (a, b, p, q) = (5.0, 6.0, 3.0, 4.0) and (5.0, 6.0, 4.0, 4.5); in the latter configuration the surface *pq* was significantly more often perceived as being in front than in the former configuration. Since they used the simple subtractive difference to predict the perceived depth order and $|b - q| - |p - q|$ gave the same value for both of these stimuli, they concluded that the contrast between figure and ground was also necessary for predicting their results. However, using the relative contrast difference ρ (Equation 10), we could explain the difference without considering any effect of the contrast against the background region: $\rho = 0.67$ in the former configuration and $\rho = 0.75$ in the latter configuration, which means that ρ predicts higher percentage "surface *pq* in front" in the latter configuration.

In previous studies, it has been shown that the observer could correctly match or rate the filter transmittance or the reflective component of simulated filters under different background conditions (Gerbino et al., 1990; Kasrai & Kingdom, 2001; Masin, 2006; Robilotto, Khang, & Zaidi, 2002; Robilotto & Zaidi, 2004; Singh & Anderson, 2002, 2006). Therefore, one possibility was that the depth ordering was judged by comparing the representations of the filter property under possible interpretations. However, such a strategy would be possible only when both of those representations are going to be ecologically plausible quantities; it would be hard to imagine a transparent filter whose transmittance value is larger than one. In our study, the interpretations of the patterns were restricted to "left disk in front" and "right disk in front" due to the figural constraints. Thus, there were cases in which either or both of those interpretations gave rise to invalid transmittance or invalid reflected luminance. In the section "The relationships between the physical photometric constraint and the perceived depth ordering," we tested a model that incorporated a strategy that compares transmittance values of the two interpretations. As expected, the model could not explain the data in cases where either or both of the transmittance values was larger than one ("*pq* and *ap* valid," "*bq* and *ab* valid," and "*ap* and *ab* valid" conditions in Figure 10B). In addition, we found that even when both of the two alternative interpretations were physically valid ("*pq* and *bq* valid" condition), the goodness of prediction by such a model was worse than that produced by the simpler model ρ in Equation 10. Since the model ρ could consistently explain the data irrespective of those physical photometric conditions, it is plausible that the visual system did not take physical filter property as a criterion to determine depth ordering in bistable transparency patterns. However, this does not necessarily mean that the human visual system cannot intrinsically estimate filter properties. We think that the results of our study indicate that the depth stratification of transparency patterns can be

solved before accurate filter-property estimation is completed. In such cases, the relative difference of contrast against a shared region will be the most important photometric factor.

Some previous studies that investigated perceived depth ordering for bistable transparency patterns have also found a similar tendency. Kitaoka (2005) classified possible interpretations of bistable transparency patterns and examined the frequency of each interpretation. Although the figural constraint in the stimulus pattern he used was not that strong, and multiple interpretations were allowed, he found the same tendency as that we found: A surface comprising two regions that have a smaller lightness difference between them tends to be perceived as being in front. Beck et al. (1984) also used a small set of bistable transparency patterns among others and suggested a similar tendency. These studies, however, did not make a model that predicts the likelihood of occurrence of each interpretation. On the other hand, in an earlier study by Oyama and Nakahara (1960), they used white and black bars crossing on a gray background (Type 2 stimulus in our definition) and examined the time course of switching of dominancy of each of the two interpretations (i.e., white in front or black in front). Thus, the stimulus configuration of their study was very similar to those of our study and that by Delogu et al. (2010) in that it induced depth rivalry between two objects in front of the background. In their study, they found that the smaller the difference in lightness between either the white or black region and the crossing (shared) region, the more often the surface comprising the two regions appeared to be in front. Moreover, they found that the lightness of the background region had little effect on the relative dominancy. Therefore, their findings match quite well with our conclusion. In our study, we confirmed this tendency using stimuli in larger dimensional space of luminance combinations and demonstrated that the model ρ can explain the data irrespective of the physical photometric conditions.

The visual system is likely to rely on lightness when perceiving depth order of transparency patterns

In line with the other previous studies (Delogu et al., 2010; Kitaoka, 2005; Oyama & Nakahara, 1960), in this study we also found that the depth-order preferences are best predicted when lightness difference was used as a metric of contrast between two regions as shown by the fitting analysis (Figure 7 and Table 1). One might argue that the comparison was not fair because the number of free parameters was different (in addition to the two parameters s and m of a sigmoid function, a translation exponent n was incorporated for the lightness contrast metric). Nevertheless, larger differences among different stimulus types found with the metrics of luminance difference and Michelson contrast (see Figure 7B, C) indicated that those metrics were not appropriate to explain the data. It is counterintuitive that the visual system behaves differently toward these artificially introduced stimulus categories. In fact, this difference among different types of stimuli can be explained as an artifact that emerges when choosing inappropriate metrics. Actually, the range of luminance level of the two disks differed between three types of stimuli due to the constraints posed by the definition of each type. For example, the two disks have to be darker than the background region for Type 1 stimuli. By contrast, they have to be brighter than the background for Type 3 stimuli. Thus, the luminance range of the regions b, p, and q was darker as a whole for Type 1 stimuli, and it was brighter for Type 3 stimuli. Because the size of contrast overestimation or underestimation by inappropriate metrics depends on the luminance level, the patterns of deviation would also differ among the types of stimuli. At any rate, the most conservative interpretation of our data is that the visual system relies on lightness contrast when perceiving the depth ordering of bistable transparency patterns.

Conclusions

In contrast to the previous study that proposed contributions of contrast against the background region to perceived depth order in bistable transparency patterns (Delogu et al. 2010), the present study demonstrated that contrast against the background region has little influence on perceived depth order compared with contrast against the region shared by two surface candidates. In addition, we found that the perceived depth ordering is well predicted by a simple model that takes into consideration only relative size of lightness difference against the shared region. The result is consistent with several previous studies that investigated the perceived depth ordering of bistable transparency patterns (Beck et al., 1984; Kitaoka, 2005; Oyama & Nakahara, 1960).

Keywords: perceptual transparency, depth stratification, bistable transparency

Acknowledgments

We thank the two anonymous reviewers and the editor for their insightful comments and suggestions,

which significantly improved the manuscript. This work was supported in part by NET (Next-generation Energies for Tohoku Recovery) Project of Ministry of Education, Culture, Sports, Science, and Technology and in part by SCOPE (Strategic Information and Communications R&D Promotion Program) of Ministry of Internal Affairs and Communications. TF was supported by Grant-in-Aid for JSPS Fellows (25-8093).

Commercial relationships: none.
Corresponding author: Taiki Fukiage.
Email: fukiage@cvl.iis.u-tokyo.ac.jp.
Address: Graduate School of Interdisciplinary Information Studies, University of Tokyo, Meguro-ku, Tokyo, Japan.

References

Adelson, E. H., & Anandan, P. (1990, July). *Ordinal characteristics of transparency*. Paper presented at the AAAI-90 Workshop on Qualitative Vision, Boston, MA.

Anderson, B. L. (1997). A theory of illusory lightness and transparency in monocular and binocular images: The role of contour junctions. *Perception, 26,* 419–454. [PubMed]

Anderson, B. L. (2003). The role of occlusion in the perception of depth, lightness, and opacity. *Psychological Review, 110,* 762–784. [PubMed]

Anderson, B. L., Singh, M., & Meng, J. (2006). The perceived transmittance of inhomogeneous surfaces and media. *Vision Research, 46,* 1982–1995. [PubMed]

Beck, J., & Ivry, R. (1988). On the role of figural organization in perceptual transparency. *Perception and Psychophysics, 44,* 585–594. [PubMed]

Beck, J., Prazdny, K., & Ivry, R. (1984). The perception of transparency with achromatic colors. *Perception and Psychophysics, 35,* 407–422. [PubMed]

Delogu, F., Fedorov, G., Belardinelli, M. O., & van Leeuwen, G. (2010). Perceptual preferences in depth stratification of transparent layers: Photometric and non-photometric factors. *Journal of Vision*, *10*(2):19, 1–13, http://www.journalofvision.org/content/10/2/19, doi:10.1167/10.2.19. [PubMed] [Article]

Gerbino, W. (1994). Achromatic transparency. In A. L. Gilchrist (Ed.), *Lightness, brightness, and transparency* (pp. 215–255). Hillsdale, NJ: Erlbaum.

Gerbino, W., Stultiens, C., Troost, J., & de Weert, C. (1990). Transparent layer constancy. *Journal of Experimental Psychology: Human Perception and Performance, 16,* 3–20. [PubMed]

Kasrai, R., & Kingdom, F. A. A. (2001). Precision, accuracy, and range of perceived achromatic transparency. *Journal of the Optical Society of America A, 18,* 1–11. [PubMed]

Kitaoka, A. (2005). A new explanation of perceptual transparency connecting the X-junction contrast-polarity model with the luminance-based arithmetic model. *Japanese Psychological Research, 47,* 175–187.

Koenderink, J., van Doorn, A. J., Pont, S. C., & Richards, W. (2008). Gestalt and phenomenal transparency. *Journal of the Optical Society of America A: Optics, Image Science, and Vision, 25,* 190–202. [PubMed]

Masin, S. C. (2006). Test of models of achromatic transparency. *Perception, 35,* 1611–1624.

Metelli, F. (1974a). Achromatic colour conditions in the perception of transparency. In R. B. MacLeod & H. L. Pick (Eds.), *Perception: Essays in honor of James J. Gibson* (pp. 95–116). Ithaca, NY: Cornell University Press.

Metelli, F. (1974b). The perception of transparency. *Scientific American, 230,* 91–98. [PubMed]

Metelli, F. (1985). Stimulation and perception of transparency. *Psychological Research, 47,* 185–202. [PubMed]

Metelli, F., Da Pos, O., & Cavedon, A. (1985). Balanced and unbalanced, complete and partial transparency. *Perception and Psychophysics, 38,* 354–366. [PubMed]

Oyama, T., & Nakahara, J. I. (1960). The effects of lightness, hue and area upon the apparent transparency. *Japanese Journal of Psychology, 31,* 35–48.

Robilotto, R., Khang, B.-G., & Zaidi, Q. (2002). Sensory and physical determinants of perceived achromatic transparency. *Journal of Vision*, *2*(5):3, 388–403, http://www.journalofvision.org/content/2/5/3, doi:10.1167/2.5.3. [PubMed] [Article]

Robilotto, R., & Zaidi, Q. (2004). Perceived transparency of neutral density filters across dissimilar backgrounds. *Journal of Vision, 4*(3)5:183–195, http://www.journalofvision.org/content/4/3/5, doi:10.1167/4.3.5. [PubMed] [Article]

Singh, M., & Anderson, B. L. (2002). Toward a perceptual theory of transparency. *Psychological Review, 109,* 492–519. [PubMed]

Singh, M., & Anderson, B. L. (2006). Photometric determinants of perceived transparency. *Vision Research, 46,* 879–894. [PubMed: http://www.ncbi.nlm.nih.gov/pubmed/16359720]

Warren, R. M., & Poulton, E. C. (1960). Basis for lightness-judgments of grays. *American Journal of Physiology, 73,* 380–387. [PubMed]

Warren, R. M., & Poulton, E. C. (1966). Lightness of grays: Effects of background reflectance. *Perception and Psychophysics, 1,* 145–148. [PubMed]

Wyszecki, G. (1963). Proposal for a new color-difference formula. *Journal of the Optical Society of America, 53,* 1318–1319.

Appendix A

A brief summary of the groups classified based on the physical photometric conditions

We classified all the stimuli based on which interpretation the photometric constraint supports. Each of the stimuli was categorized into five groups depending on whether it satisfied rules 2 and 3 of the photometric constraint as described in the section "The relationships between the physical photometric constraint and the perceived depth ordering." Those groups were termed "*pq* and *bq* valid," "*pq* and *ap* valid," "*bq* and *ab* valid," "*ap* and *ab* valid," and "all invalid." In the second column of Table 4, we showed the number of the stimuli and the averaged percentage of canceled trials in each group. As for the data of percentage "left in front," we showed the histogram for each group in Figure 11.

In the third to fifth columns termed Type 1, Type 2, and Type 3 in Table 4, we showed the same statistics calculated within each stimulus type defined in Figure 4. In Type 1 stimuli, any stimulus was not classified into either "*pq* and *ap* valid" or "*bq* and *ab* valid" groups. This is because if a stimulus in Type 1 satisfies rule 2 under the "surface *pq* in front" assumption (i.e., $a - b > p - q$), it also satisfies rule 2 under the "surface *bq* in front" assumption (i.e., $a - p > b - q$) and does not satisfy rule 2 under the other assumptions. By contrast, if a stimulus in Type 1 does not satisfy rule 2 under the "surface *pq* in front" assumption (i.e., $a - b < p - q$), it also doesn't satisfy rule 2 under the "surface *bq* in front" assumption (i.e., $a - p < b - q$) and does satisfy rule 2 under the other assumptions. Thus, there is no theoretical room for Type 1 stimuli to satisfy both the *pq*-valid and *ap*-valid constraints or both the *bq*-valid and *ab*-valid constraints. For the same reason, it can theoretically be said that any stimulus in Type 2 is not classified into either the "*pq* and *bq* valid" or "*ab* and *ap* valid" groups and that any stimulus in Type 3 is not classified into either the "*pq* and *ap* valid" or "*bq* and *ab* valid" groups.

The relationships between the physical photometric constraint and the percentage of canceled trials

The percentage of canceled trials was quite low for every stimulus (2.8% on average, 22.2% at most). This indicated that figural constraint in the present study was strong enough to overcome the photometric constraint. Thus, we did not focus on the percentages of canceled trials in the main part of this study. Nevertheless, one can expect that the canceled trials might increase in those trials in which both of the "left (surface *pq*) in front" answer and the "right (surface *bq*) in front" answer were inconsistent with the physical photometric constraints. To test this hypothesis, we examined whether the percentage of canceled trials was larger in the "*ap* and *ab* valid" group or in the "all invalid" group. We conducted

	All		Type 1		Type 2		Type 3	
Group	Stimuli (*N*)	Canceled trials (%)	Stimuli (*N*)	Canceled trials (%)	Stimuli (*N*)	Canceled trials (%)	Stimuli (*N*)	Canceled trials (%)
pq and *bq* valid	116	3.57	70	2.58	0	–	46	5.07
pq and *ap* valid	38	1.54	0	–	38	1.54	0	–
bq and *ab* valid	38	0.44	0	–	38	0.44	0	–
ap and *ab* valid	40	6.88	14	1.98	0	–	26	9.51
All invalid	330	2.44	96	1.22	132	0.59	102	5.99

Table 4. The number of stimuli and the averaged percentage of canceled trials in each group classified based on the physical photometric constraint. "*pq* and *bq* valid" indicates the group in which the "surface *pq* in front" and the "surface *bq* in front" interpretations are both photometrically valid; "all invalid" indicates the group in which all of the four interpretations (*pq* in front, *bq* in front, *ap* in front, and *ab* in front) are photometrically invalid. The columns termed Type 1, Type 2, and Type 3 show the statistics calculated within each stimulus type defined in Figure 4. A dash (–) indicates that the averaged percentage of canceled trials were not available.

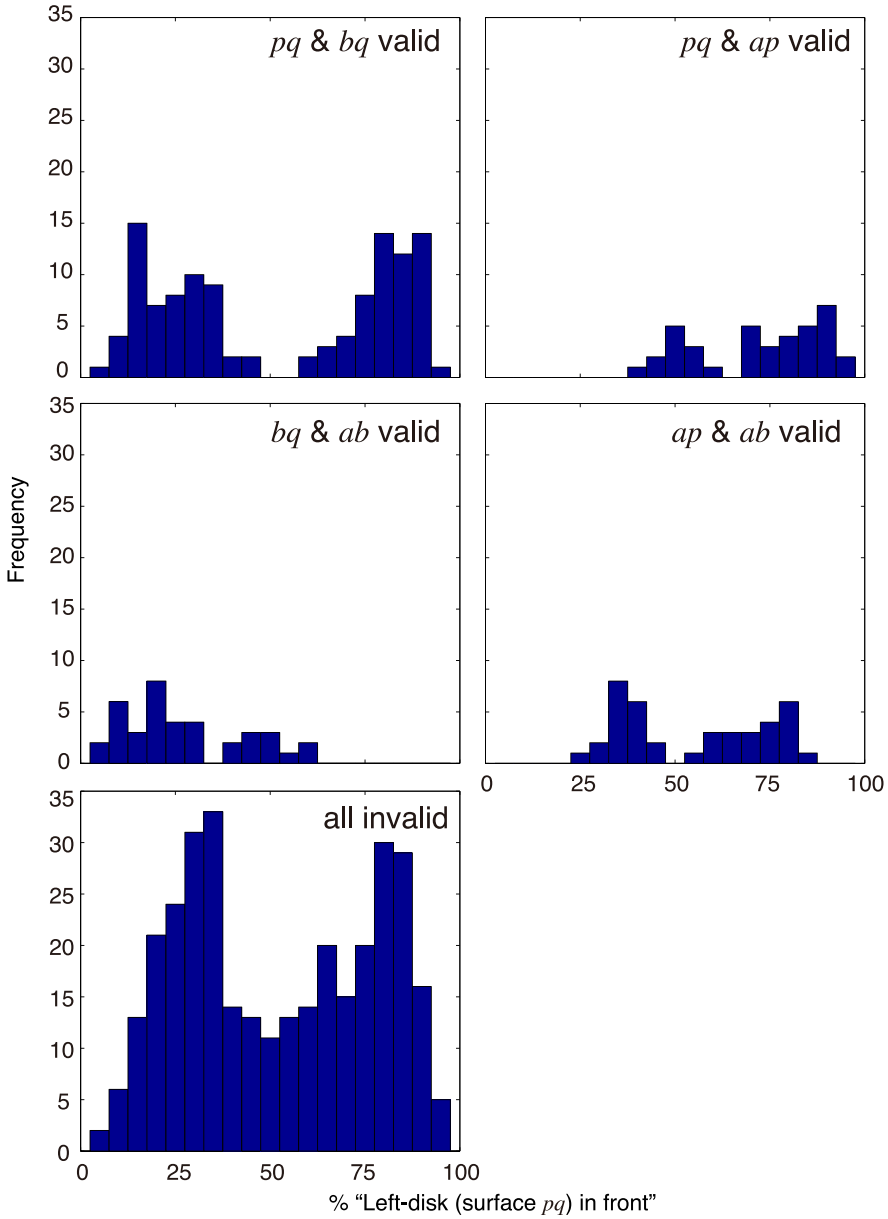

Figure 11. The histograms of percentage "left (surface *pq*) in front" for each group classified based on the physical photometric constraint.

one-way ANOVA (analysis of variance) for the data of each stimulus type, but we could not find any tendency that the percentage of canceled trials in the "all invalid" group was larger than that in the other groups. On the other hand, only in the data of Type 3 stimulus did we find a significant increase in the percentage of canceled trials in the "*ap* and *ab* valid" group compared with the "*pq* and *bq* valid" ($p < 0.0001$) and the "all invalid" ($p < 0.001$) groups as a result of multiple comparisons (Tukey's honest significant difference test) following one-way ANOVA [$F(2, 171) = 10.2$, $p < 0.001$)]. Therefore, the hypothesis that the percentage of canceled trials follows physical photometric constraint was partially supported. However, this does not indicate that the visual system relies on the physical photometric constraint because the visual system might use another criterion (e.g., ρ in Equation 10) that is different yet somewhat similar and covaries with the physical photometric constraint. Because the number of canceled trials was low and we could not know what kind of interpretation the observers actually perceived in those trials, we could not obtain further information from the canceled trials.

Appendix B

#	Stimulus type	Luminance					Left in front (%)	Canceled trials (%)
		a	*b*	*p*	*q*	ρ		
1	1	89.8	2	67.8	0.8	−0.857	19.4	0
2	1	89.8	2	49.8	0.8	−0.833	22.2	0
3	1	89.8	2	35.3	0.8	−0.802	14.3	2.8
4	1	49.8	2	35.3	0.8	−0.802	16.7	0
5	1	89.8	2	23.9	0.8	−0.759	16.7	0
6	1	49.8	2	23.9	0.8	−0.759	13.9	0
7	1	89.8	9	67.8	4.7	−0.748	22.2	0
8	1	89.8	35.3	49.8	32.9	−0.733	17.1	2.8
9	1	89.8	49.8	67.8	46.7	−0.722	22.9	2.8
10	1	89.8	23.9	35.3	22	−0.718	14.7	5.6
11	1	49.8	23.9	35.3	22	−0.718	11.1	0
12	1	49.8	15.3	23.9	13.7	−0.702	17.1	2.8
13	1	89.8	9	49.8	4.7	−0.698	27.8	0
14	1	89.8	2	15.3	0.8	−0.696	13.9	0
15	1	49.8	2	15.3	0.8	−0.696	11.4	2.8
16	1	23.9	2	15.3	0.8	−0.696	13.9	0
17	1	89.8	4.7	67.8	0.8	−0.683	22.2	0
18	1	89.8	4.7	49.8	0.8	−0.637	11.1	0
19	1	89.8	9	35.3	4.7	−0.628	27.8	0
20	1	49.8	9	35.3	4.7	−0.628	25	0
21	1	89.8	23.9	67.8	15.3	−0.624	19.4	0
22	1	89.8	2	9	0.8	−0.597	17.1	2.8
23	1	49.8	2	9	0.8	−0.597	13.9	0
24	1	23.9	2	9	0.8	−0.597	33.3	0
25	1	89.8	4.7	35.3	0.8	−0.577	8.3	0
26	1	49.8	4.7	35.3	0.8	−0.577	37.1	2.8
27	1	89.8	15.3	67.8	4.7	−0.541	25	0
28	1	89.8	9	67.8	0.8	−0.532	27.8	0
29	1	89.8	9	23.9	4.7	−0.523	20	2.8
30	1	49.8	9	23.9	4.7	−0.523	22.2	0
31	1	89.8	23.9	49.8	15.3	−0.519	25	0
32	1	89.8	35.3	49.8	29.4	−0.516	34.3	2.8
33	1	89.8	23.9	35.3	19.2	−0.506	22.2	0
34	1	49.8	23.9	35.3	19.2	−0.506	25	0
35	1	89.8	49.8	67.8	42	−0.502	34.3	2.8
36	1	49.8	15.3	23.9	11.8	−0.501	19.4	0
37	1	89.8	4.7	23.9	0.8	−0.498	33.3	0
38	1	49.8	4.7	23.9	0.8	−0.498	19.4	0
39	1	89.8	9	49.8	0.8	−0.47	30.6	0
40	1	89.8	15.3	49.8	4.7	−0.463	38.9	0
41	1	89.8	2	4.7	0.8	−0.419	16.7	16.7
42	1	49.8	2	4.7	0.8	−0.419	18.2	8.3
43	1	23.9	2	4.7	0.8	−0.419	17.1	2.8
44	1	9	2	4.7	0.8	−0.419	28.6	2.8
45	1	6.7	2	4.7	0.8	−0.419	22.2	0
46	1	15.3	2	4.7	0.8	−0.419	28.6	2.8
47	1	89.8	9	35.3	0.8	−0.393	33.3	0
48	1	49.8	9	35.3	0.8	−0.393	31.4	2.8
49	1	89.8	4.7	15.3	0.8	−0.391	31.4	2.8

#	Stimulus type	Luminance					Left in front (%)	Canceled trials (%)
		a	*b*	*p*	*q*	ρ		
50	1	49.8	4.7	15.3	0.8	−0.391	19.4	0
51	1	23.9	4.7	15.3	0.8	−0.391	13.9	0
52	1	89.8	23.9	67.8	4.7	−0.369	22.9	2.8
53	1	89.8	15.3	35.3	4.7	−0.36	33.3	0
54	1	49.8	15.3	35.3	4.7	−0.36	36.1	0
55	1	89.8	35.3	67.8	15.3	−0.355	14.3	2.8
56	1	89.8	9	15.3	4.7	−0.347	25.7	2.8
57	1	49.8	9	15.3	4.7	−0.347	40	2.8
58	1	23.9	9	15.3	4.7	−0.347	42.9	2.8
59	1	19.2	9	15.3	4.7	−0.347	36.1	0
60	1	35.3	9	15.3	4.7	−0.347	29.4	5.6
61	1	67.8	9	15.3	4.7	−0.347	34.3	2.8
62	1	49.8	15.3	23.9	9	−0.346	31.4	2.8
63	1	89.8	23.9	35.3	15.3	−0.345	34.3	2.8
64	1	49.8	23.9	35.3	15.3	−0.345	37.1	2.8
65	1	42	23.9	35.3	15.3	−0.345	27.8	0
66	1	67.8	23.9	35.3	15.3	−0.345	28.6	2.8
67	1	89.8	35.3	49.8	23.9	−0.344	33.3	0
68	1	89.8	49.8	67.8	35.3	−0.343	36.1	0
69	1	89.8	9	23.9	0.8	−0.296	33.3	0
70	1	49.8	9	23.9	0.8	−0.296	14.3	2.8
71	1	89.8	23.9	49.8	4.7	−0.276	33.3	0
72	1	89.8	4.7	9	0.8	−0.237	35.3	5.6
73	1	49.8	4.7	9	0.8	−0.237	44.4	0
74	1	23.9	4.7	9	0.8	−0.237	31.4	2.8
75	1	89.8	35.3	67.8	4.7	−0.225	40	2.8
76	1	89.8	15.3	23.9	4.7	−0.215	45.7	2.8
77	1	49.8	15.3	23.9	4.7	−0.215	37.1	2.8
78	1	89.8	23.9	35.3	9	−0.213	36.1	0
79	1	49.8	23.9	35.3	9	−0.213	38.9	0
80	1	89.8	35.3	49.8	15.3	−0.212	25	0
81	1	89.8	49.8	67.8	23.9	−0.211	41.2	5.6
82	1	89.8	9	15.3	0.8	−0.17	37.1	2.8
83	1	49.8	9	15.3	0.8	−0.17	47.1	5.6
84	1	23.9	9	15.3	0.8	−0.17	30.6	0
85	1	49.8	15.3	23.9	2	−0.158	34.3	2.8
86	1	89.8	23.9	35.3	4.7	−0.157	48.6	2.8
87	1	49.8	23.9	35.3	4.7	−0.157	41.7	0
88	1	89.8	35.3	49.8	9	−0.156	42.9	2.8
89	1	89.8	49.8	67.8	15.3	−0.154	29.4	5.6
90	1	89.8	35.3	49.8	4.7	−0.125	42.9	2.8
91	1	89.8	49.8	35.3	4.7	0.125	65.7	2.8
92	1	89.8	67.8	49.8	15.3	0.154	71.4	2.8
93	1	89.8	49.8	35.3	9	0.156	50	0
94	1	89.8	35.3	23.9	4.7	0.157	74.3	2.8
95	1	49.8	35.3	23.9	4.7	0.157	60	2.8
96	1	49.8	23.9	15.3	2	0.158	69.4	0
97	1	89.8	15.3	9	0.8	0.17	56.3	11.1
98	1	49.8	15.3	9	0.8	0.17	55.9	5.6
99	1	23.9	15.3	9	0.8	0.17	68.6	2.8
100	1	89.8	67.8	49.8	23.9	0.211	64.7	5.6
101	1	89.8	49.8	35.3	15.3	0.212	60	2.8
102	1	89.8	35.3	23.9	9	0.213	64.7	5.6

#	Stimulus type	Luminance					Left in front (%)	Canceled trials (%)
		a	*b*	*p*	*q*	ρ		
103	1	49.8	35.3	23.9	9	0.213	58.3	0
104	1	89.8	23.9	15.3	4.7	0.215	61.8	5.6
105	1	49.8	23.9	15.3	4.7	0.215	50	0
106	1	89.8	67.8	35.3	4.7	0.225	69.4	0
107	1	89.8	9	4.7	0.8	0.237	62.5	11.1
108	1	49.8	9	4.7	0.8	0.237	65.7	2.8
109	1	23.9	9	4.7	0.8	0.237	74.3	2.8
110	1	89.8	49.8	23.9	4.7	0.276	69.4	0
111	1	89.8	23.9	9	0.8	0.296	75	0
112	1	49.8	23.9	9	0.8	0.296	80	2.8
113	1	89.8	67.8	49.8	35.3	0.343	63.9	0
114	1	89.8	49.8	35.3	23.9	0.344	72.2	0
115	1	89.8	35.3	23.9	15.3	0.345	79.4	5.6
116	1	49.8	35.3	23.9	15.3	0.345	57.1	2.8
117	1	42	35.3	23.9	15.3	0.345	69.4	0
118	1	67.8	35.3	23.9	15.3	0.345	79.4	5.6
119	1	49.8	13.9	15.3	9	0.346	68.6	2.8
120	1	89.8	15.3	9	4.7	0.347	82.4	5.6
121	1	49.8	15.3	9	4.7	0.347	80	2.8
122	1	23.9	15.3	9	4.7	0.347	63.9	0
123	1	19.2	15.3	9	4.7	0.347	77.1	2.8
124	1	35.3	15.3	9	4.7	0.347	62.9	2.8
125	1	67.8	15.3	9	4.7	0.347	61.8	5.6
126	1	89.8	67.8	35.3	15.3	0.355	83.3	0
127	1	89.8	35.3	15.3	4.7	0.36	63.9	0
128	1	49.8	35.3	15.3	4.7	0.36	65.7	2.8
129	1	89.8	67.8	23.9	4.7	0.369	66.7	0
130	1	89.8	15.3	4.7	0.8	0.391	82.9	2.8
131	1	49.8	15.3	4.7	0.8	0.391	80.6	0
132	1	23.9	15.3	4.7	0.8	0.391	77.8	0
133	1	89.8	35.3	9	0.8	0.393	75	0
134	1	49.8	35.3	9	0.8	0.393	77.8	0
135	1	89.8	4.7	2	0.8	0.419	82.9	2.8
136	1	49.8	4.7	2	0.8	0.419	77.4	13.9
137	1	23.9	4.7	2	0.8	0.419	80.6	0
138	1	9	4.7	2	0.8	0.419	80.6	0
139	1	6.7	4.7	2	0.8	0.419	73.5	5.6
140	1	15.3	4.7	2	0.8	0.419	75	0
141	1	89.8	49.8	15.3	4.7	0.463	71.4	2.8
142	1	89.8	49.8	9	0.8	0.47	63.9	0
143	1	89.8	23.9	4.7	0.8	0.498	86.1	0
144	1	49.8	23.9	4.7	0.8	0.498	75	0
145	1	49.8	23.9	15.3	11.8	0.501	75	0
146	1	89.8	67.8	49.8	42	0.502	69.4	0
147	1	89.8	35.3	23.9	19.2	0.506	75	0
148	1	49.8	35.3	23.9	19.2	0.506	73.5	5.6
149	1	89.8	49.8	35.3	29.4	0.516	83.3	0
150	1	89.8	49.8	23.9	15.3	0.519	86.1	0
151	1	89.8	23.9	9	4.7	0.523	77.8	0
152	1	49.8	23.9	9	4.7	0.523	80	2.8
153	1	89.8	67.8	9	0.8	0.532	86.1	0
154	1	89.8	67.8	15.3	4.7	0.541	80.6	0
155	1	89.8	35.3	4.7	0.8	0.577	86.1	0

#	Stimulus type	Luminance					Left in front (%)	Canceled trials (%)
		a	*b*	*p*	*q*	ρ		
156	1	49.8	35.3	4.7	0.8	0.577	75	0
157	1	89.8	9	2	0.8	0.597	88.9	0
158	1	49.8	9	2	0.8	0.597	80.6	0
159	1	23.9	9	2	0.8	0.597	77.8	0
160	1	89.8	67.8	23.9	15.3	0.624	86.1	0
161	1	89.8	35.3	9	4.7	0.628	80	2.8
162	1	49.8	35.3	9	4.7	0.628	81.8	8.3
163	1	89.8	49.8	4.7	0.8	0.637	91.7	0
164	1	89.8	67.8	4.7	0.8	0.683	86.1	0
165	1	89.8	15.3	2	0.8	0.696	88.9	0
166	1	49.8	15.3	2	0.8	0.696	86.1	0
167	1	23.9	15.3	2	0.8	0.696	83.3	0
168	1	89.8	49.8	9	4.7	0.698	80.6	0
169	1	49.8	23.9	15.3	13.7	0.702	91.4	2.8
170	1	89.8	35.3	23.9	22	0.718	88.6	2.8
171	1	49.8	35.3	23.9	22	0.718	83.3	0
172	1	89.8	67.8	49.8	46.7	0.722	88.2	5.6
173	1	89.8	49.8	35.3	32.9	0.733	91.4	2.8
174	1	89.8	67.8	9	4.7	0.748	83.3	0
175	1	89.8	23.9	2	0.8	0.759	88.9	0
176	1	49.8	23.9	2	0.8	0.759	88.9	0
177	1	89.8	35.3	2	0.8	0.802	88.9	0
178	1	49.8	35.3	2	0.8	0.802	94.4	0
179	1	89.8	49.8	2	0.8	0.833	88.9	0
180	1	89.8	67.8	2	0.8	0.857	86.1	0
181	2	4.7	0.8	49.8	2	−0.818	19.4	0
182	2	9	0.8	49.8	2	−0.818	17.1	2.8
183	2	15.3	0.8	49.8	2	−0.818	2.8	0
184	2	23.9	0.8	49.8	2	−0.818	5.6	0
185	2	35.3	0.8	49.8	2	−0.818	11.1	0
186	2	15.3	4.7	89.8	9	−0.758	13.9	0
187	2	23.9	4.7	89.8	9	−0.758	16.7	0
188	2	35.3	4.7	89.8	9	−0.758	8.3	0
189	2	49.8	4.7	89.8	9	−0.758	16.7	0
190	2	67.8	4.7	89.8	9	−0.758	5.6	0
191	2	4.7	0.8	23.9	2	−0.726	11.1	0
192	2	9	0.8	23.9	2	−0.726	8.3	0
193	2	15.3	0.8	23.9	2	−0.726	11.1	0
194	2	9	89.8	4.7	67.8	−0.673	30.6	0
195	2	15.3	89.8	4.7	67.8	−0.673	13.9	0
196	2	23.9	89.8	4.7	67.8	−0.673	19.4	0
197	2	35.3	89.8	4.7	67.8	−0.673	11.1	0
198	2	49.8	89.8	4.7	67.8	−0.673	11.1	0
199	2	2	49.8	0.8	35.3	−0.655	33.3	0
200	2	4.7	49.8	0.8	35.3	−0.655	19.4	0
201	2	9	49.8	0.8	35.3	−0.655	25	0
202	2	15.3	49.8	0.8	35.3	−0.655	22.2	0
203	2	23.9	49.8	0.8	35.3	−0.655	22.2	0
204	2	15.	4.7	49.8	9	−0.645	19.4	0
205	2	23.9	4.7	49.8	9	−0.645	5.6	0
206	2	35.3	4.7	49.8	9	−0.645	25	0
207	2	35.3	15.3	89.8	23.9	−0.637	11.1	0
208	2	49.8	15.3	89.8	23.9	−0.637	22.2	0

#	Stimulus type	Luminance					Left in front (%)	Canceled trials (%)
		a	*b*	*p*	*q*	ρ		
209	2	67.8	15.3	89.8	23.9	−0.637	16.7	0
210	2	23.9	89.8	15.3	67.8	−0.565	27.8	0
211	2	35.3	89.8	15.3	67.8	−0.565	27.8	0
212	2	49.8	89.8	15.3	67.8	−0.565	19.4	0
213	2	9	49.8	4.7	35.3	−0.557	25	0
214	2	15.3	49.8	4.7	35.3	−0.557	36.1	0
215	2	23.9	49.8	4.7	35.3	−0.557	25	0
216	2	2	0.8	49.8	4.7	−0.556	27.8	0
217	2	9	0.8	49.8	4.7	−0.556	16.7	0
218	2	15.3	0.8	49.8	4.7	−0.556	8.3	0
219	2	23.9	0.8	49.8	4.7	−0.556	13.9	0
220	2	35.3	0.8	49.8	4.7	−0.556	19.4	0
221	2	2	23.9	0.8	15.3	−0.53	25	0
222	2	4.7	23.9	0.8	15.3	−0.53	30.6	0
223	2	9	23.9	0.8	15.3	−0.53	22.9	2.8
224	2	9	4.7	89.8	15.3	−0.502	22.2	0
225	2	23.9	4.7	89.8	15.3	−0.502	25	0
226	2	35.3	4.7	89.8	15.3	−0.502	25.7	2.8
227	2	49.8	4.7	89.8	15.3	−0.502	16.7	0
228	2	67.8	4.7	89.8	15.3	−0.502	22.2	0
229	2	4.7	0.8	9	2	−0.496	33.3	0
230	2	15.3	4.7	23.9	9	−0.373	25	0
231	2	35.3	15.3	49.8	23.9	−0.367	22.2	0
232	2	67.8	35.3	89.8	49.8	−0.361	27.8	0
233	2	9	89.8	4.7	49.8	−0.359	24.2	8.3
234	2	15.3	89.8	4.7	49.8	−0.359	27.8	0
235	2	23.9	89.8	4.7	49.8	−0.359	40	2.8
236	2	35.3	89.8	4.7	49.8	−0.359	33.3	0
237	2	67.8	89.8	4.7	49.8	−0.359	22.9	2.8
238	2	2	0.8	23.9	4.7	−0.33	30.6	0
239	2	9	0.8	23.9	4.7	−0.33	30.6	0
240	2	15.3	0.8	23.9	4.7	−0.33	25	0
241	2	2	49.8	0.8	23.9	−0.327	36.1	0
242	2	4.7	49.8	0.8	23.9	−0.327	31.4	2.8
243	2	9	49.8	0.8	23.9	−0.327	41.7	0
244	2	15.3	49.8	0.8	23.9	−0.327	41.7	0
245	2	35.3	49.8	0.8	23.9	−0.327	22.2	0
246	2	49.8	89.8	35.3	67.8	−0.307	38.9	0
247	2	23.9	49.8	15.3	35.3	−0.3	41.7	0
248	2	9	23.9	4.7	15.3	−0.293	27.8	0
249	2	2	0.8	49.8	9	−0.279	38.9	0
250	2	4.7	0.8	49.8	9	−0.279	25	0
251	2	15.3	0.8	49.8	9	−0.279	33.3	0
252	2	23.9	0.8	49.8	9	−0.279	25	0
253	2	35.3	0.8	49.8	9	−0.279	36.1	0
254	2	9	4.7	49.8	15.3	−0.267	27.8	0
255	2	23.9	4.7	49.8	15.3	−0.267	41.7	0
256	2	35.3	4.7	49.8	15.3	−0.267	36.1	0
257	2	23.9	15.3	89.8	35.3	−0.255	44.4	0
258	2	49.8	15.3	89.8	35.3	−0.255	27.8	0
259	2	67.8	15.3	89.8	35.3	−0.255	38.9	0
260	2	2	9	0.8	4.7	−0.233	33.3	0
261	2	9	4.7	89.8	23.9	−0.229	31.4	2.8

#	Stimulus type	Luminance					Left in front (%)	Canceled trials (%)
		a	*b*	*p*	*q*	ρ		
262	2	15.3	4.7	89.8	23.9	−0.229	25.7	2.8
263	2	35.3	4.7	89.8	23.9	−0.229	27.8	0
264	2	49.8	4.7	89.8	23.9	−0.229	30.6	0
265	2	67.8	4.7	89.8	23.9	−0.229	33.3	0
266	2	23.9	89.8	15.3	49.8	−0.147	38.9	0
267	2	35.3	89.8	15.3	49.8	−0.147	35.3	5.6
268	2	67.8	89.8	15.3	49.8	−0.147	41.7	0
269	2	9	49.8	4.7	23.9	−0.134	48.6	2.8
270	2	15.3	49.8	4.7	23.9	−0.134	37.1	2.8
271	2	35.3	49.8	4.7	23.9	−0.134	47.2	0
272	2	2	23.9	0.8	9	−0.086	50	0
273	2	4.7	23.9	0.8	9	−0.086	42.9	2.8
274	2	15.3	23.9	0.8	9	−0.086	44.4	0
275	2	9	89.8	4.7	35.3	−0.058	47.1	5.6
276	2	15.3	89.8	4.7	35.3	−0.058	40	2.8
277	2	23.9	89.8	4.7	35.3	−0.058	44.4	0
278	2	49.8	89.8	4.7	35.3	−0.058	41.7	0
279	2	67.8	89.8	4.7	35.3	−0.058	52.8	0
280	2	2	49.8	0.8	15.3	−0.015	51.4	2.8
281	2	4.7	49.8	0.8	15.3	−0.015	36.1	0
282	2	9	49.8	0.8	15.3	−0.015	50	5.6
283	2	23.9	49.8	0.8	15.3	−0.015	62.9	2.8
284	2	35.3	49.8	0.8	15.3	−0.015	47.2	0
285	2	2	0.8	49.8	15.3	0.015	51.4	2.8
286	2	4.7	0.8	49.8	15.3	0.015	67.6	5.6
287	2	9	0.8	49.8	15.3	0.015	58.3	0
288	2	23.9	0.8	49.8	15.3	0.015	41.7	0
289	2	35.3	0.8	49.8	15.3	0.015	50	0
290	2	9	4.7	89.8	35.3	0.058	58.3	0
291	2	15.3	4.7	89.8	35.3	0.058	61.1	0
292	2	23.9	4.7	89.8	35.3	0.058	58.3	0
293	2	49.8	4.7	89.8	35.3	0.058	41.7	0
294	2	67.8	4.7	89.8	35.3	0.058	47.2	0
295	2	2	0.8	23.9	9	0.086	58.3	0
296	2	4.7	0.8	23.9	9	0.086	52.8	0
297	2	15.3	0.8	23.9	9	0.086	55.6	0
298	2	9	4.7	49.8	23.9	0.134	48.6	2.8
299	2	15.3	4.7	49.8	23.9	0.134	65.7	2.8
300	2	35.3	4.7	49.8	23.9	0.134	72.2	0
301	2	23.9	15.3	89.8	49.8	0.147	50	0
302	2	35.3	15.3	89.8	49.8	0.147	50	0
303	2	67.8	15.3	89.8	49.8	0.147	55.6	0
304	2	9	89.8	4.7	23.9	0.229	54.3	2.8
305	2	15.3	89.8	4.7	23.9	0.229	48.6	2.8
306	2	35.3	89.8	4.7	23.9	0.229	58.3	0
307	2	49.8	89.8	4.7	23.9	0.229	47.2	0
308	2	67.8	89.8	4.7	23.9	0.229	50	0
309	2	2	0.8	9	4.7	0.233	66.7	0
310	2	23.9	89.8	15.3	35.3	0.255	68.6	2.8
311	2	49.8	89.8	15.3	35.3	0.255	55.6	0
312	2	67.8	89.8	15.3	35.3	0.255	66.7	0
313	2	9	49.8	4.7	15.3	0.267	58.8	5.6
314	2	23.9	49.8	4.7	15.3	0.267	62.9	2.8

#	Stimulus type	Luminance					Left in front (%)	Canceled trials (%)
		a	*b*	*p*	*q*	ρ		
315	2	35.3	49.8	4.7	15.3	0.267	52.8	0
316	2	2	49.8	0.8	9	0.279	73.5	5.6
317	2	4.7	49.8	0.8	9	0.279	69.4	0
318	2	15.3	49.8	0.8	9	0.279	68.6	2.8
319	2	23.9	49.8	0.8	9	0.279	65.7	2.8
320	2	35.3	49.8	0.8	9	0.279	61.1	0
321	2	9	4.7	23.9	15.3	0.293	58.3	0
322	2	23.9	15.3	49.8	35.3	0.3	58.3	0
323	2	49.8	35.3	89.8	67.8	0.307	61.1	0
324	2	2	0.8	49.8	23.9	0.327	57.1	2.8
325	2	4.7	0.8	49.8	23.9	0.327	61.1	0
326	2	9	0.8	49.8	23.9	0.327	63.9	0
327	2	15.3	0.8	49.8	23.9	0.327	68.6	2.8
328	2	35.3	0.8	49.8	23.9	0.327	75	0
329	2	2	23.9	0.8	4.7	0.33	57.1	2.8
330	2	9	23.9	0.8	4.7	0.33	63.9	0
331	2	15.3	23.9	0.8	4.7	0.33	72.2	0
332	2	9	4.7	89.8	49.8	0.359	62.9	2.8
333	2	15.3	4.7	89.8	49.8	0.359	75	0
334	2	23.9	4.7	89.8	49.8	0.359	70.6	5.6
335	2	35.3	4.7	89.8	49.8	0.359	77.1	2.8
336	2	67.8	4.7	89.8	49.8	0.359	69.4	0
337	2	67.8	89.8	35.3	49.8	0.361	69.4	0
338	2	35.3	49.8	15.3	23.9	0.367	66.7	0
339	2	15.3	23.9	4.7	9	0.373	61.1	0
340	2	4.7	9	0.8	2	0.496	80.6	0
341	2	9	89.8	4.7	15.3	0.502	68.6	2.8
342	2	23.9	89.8	4.7	15.3	0.502	68.6	2.8
343	2	35.3	89.8	4.7	15.3	0.502	80	2.8
344	2	49.8	89.8	4.7	15.3	0.502	77.8	0
345	2	67.8	89.8	4.7	15.3	0.502	75	0
346	2	2	0.8	23.9	15.3	0.53	75	0
347	2	4.7	0.8	23.9	15.3	0.53	77.8	0
348	2	9	0.8	23.9	15.3	0.53	88.9	0
349	2	2	49.8	0.8	4.7	0.556	75.8	8.3
350	2	9	49.8	0.8	4.7	0.556	77.8	0
351	2	15.3	49.8	0.8	4.7	0.556	77.8	0
352	2	23.9	49.8	0.8	4.7	0.556	86.1	0
353	2	35.3	49.8	0.8	4.7	0.556	86.1	0
354	2	9	4.7	49.8	35.3	0.557	69.4	0
355	2	15.3	4.7	49.8	35.3	0.557	80.6	0
356	2	23.9	4.7	49.8	35.3	0.557	86.1	0
357	2	23.9	15.3	89.8	67.8	0.565	80.6	0
358	2	35.3	15.3	89.8	67.8	0.565	83.3	0
359	2	49.8	15.3	89.8	67.8	0.565	77.8	0
360	2	35.3	89.8	15.3	23.9	0.637	83.3	0
361	2	49.8	89.8	15.3	23.9	0.637	91.7	0
362	2	67.8	89.8	15.3	23.9	0.637	83.3	0
363	2	15.3	49.8	4.7	9	0.645	91.2	5.6
364	2	23.9	49.8	4.7	9	0.645	77.8	0
365	2	35.3	49.8	4.7	9	0.645	77.8	0
366	2	2	0.8	49.8	35.3	0.655	77.8	0
367	2	4.7	0.8	49.8	35.3	0.655	86.1	0

#	Stimulus type	Luminance					Left in front (%)	Canceled trials (%)
		a	*b*	*p*	*q*	ρ		
368	2	9	0.8	49.8	35.3	0.655	86.1	0
369	2	15.3	0.8	49.8	35.3	0.655	91.7	0
370	2	23.9	0.8	49.8	35.3	0.655	80.6	0
371	2	9	4.7	89.8	67.8	0.673	80.6	0
372	2	15.3	4.7	89.8	67.8	0.673	80.6	0
373	2	23.9	4.7	89.8	67.8	0.673	83.3	0
374	2	35.3	4.7	89.8	67.8	0.673	91.7	0
375	2	49.8	4.7	89.8	67.8	0.673	77.8	0
376	2	4.7	23.9	0.8	2	0.726	86.1	0
377	2	9	23.9	0.8	2	0.726	91.7	0
378	2	15.3	23.9	0.8	2	0.726	88.9	0
379	2	15.3	89.8	4.7	9	0.758	88.6	2.8
380	2	23.9	89.8	4.7	9	0.758	83.3	0
381	2	35.3	89.8	4.7	9	0.758	86.1	0
382	2	49.8	89.8	4.7	9	0.758	75	0
383	2	67.8	89.8	4.7	9	0.758	86.1	0
384	2	4.7	49.8	0.8	2	0.818	94.4	0
385	2	9	49.8	0.8	2	0.818	91.4	2.8
386	2	15.3	49.8	0.8	2	0.818	97.2	0
387	2	23.9	49.8	0.8	2	0.818	94.4	0
388	2	35.3	49.8	0.8	2	0.818	97.2	0
389	3	0.8	67.8	2	89.8	−0.744	25	0
390	3	0.8	67.8	2	89.8	−0.719	25	0
391	3	4.7	23.9	15.3	25.9	−0.716	17.1	2.8
392	3	4.7	15.3	9	16.9	−0.701	5.7	2.8
393	3	15.3	35.3	23.9	38	−0.7	12.1	8.3
394	3	4.7	35.3	23.9	38	−0.7	14.3	2.8
395	3	15.3	49.8	35.3	53.3	−0.696	15.2	8.3
396	3	0.8	67.8	9	89.8	−0.687	8.6	2.8
397	3	4.7	67.8	9	89.8	−0.687	17.1	2.8
398	3	0.8	35.3	2	49.8	−0.681	19.4	0
399	3	0.8	67.8	15.3	89.8	−0.643	19.4	0
400	3	4.7	67.8	15.3	89.8	−0.643	25	0
401	3	0.8	35.3	4.7	49.8	−0.637	22.9	2.8
402	3	0.8	67.8	23.9	89.8	−0.58	8.8	5.6
403	3	4.7	67.8	23.9	89.8	−0.58	17.6	5.6
404	3	15.3	67.8	23.9	89.8	−0.58	30.6	0
405	3	0.8	35.3	9	49.8	−0.576	19.4	0
406	3	4.7	35.3	9	49.8	−0.576	20	2.8
407	3	0.8	15.3	2	23.9	−0.572	20	2.8
408	3	0.8	49.8	2	89.8	−0.553	28.6	2.8
409	3	0.8	49.8	4.7	89.8	−0.515	25.7	2.8
410	3	15.3	35.3	23.9	42	−0.497	26.5	5.6
411	3	4.7	35.3	23.9	42	−0.497	14.3	2.8
412	3	4.7	15.3	9	19.2	−0.493	14.7	5.6
413	3	15.3	49.8	35.3	58.4	−0.49	18.2	8.3
414	3	0.8	67.8	35.3	89.8	−0.485	20	2.8
415	3	4.7	67.8	35.3	89.8	−0.485	23.5	5.6
416	3	15.3	67.8	35.3	89.8	−0.485	37.1	2.8
417	3	4.7	23.9	15.3	49.4	−0.482	26.5	5.6
418	3	0.8	35.3	15.3	49.8	−0.482	26.5	5.6
419	3	4.7	35.3	15.3	49.8	−0.482	34.3	2.8
420	3	0.8	15.3	4.7	23.9	−0.478	31.4	2.8

#	Stimulus type	Luminance					Left in front (%)	Canceled trials (%)
		a	*b*	*p*	*q*	ρ		
421	3	0.8	49.8	9	89.8	−0.466	24.2	8.3
422	3	4.7	49.8	9	89.8	−0.466	17.6	5.6
423	3	0.8	23.9	2	49.8	−0.459	36.4	8.3
424	3	0.8	35.3	2	89.8	−0.406	36.4	8.3
425	3	0.8	49.8	15.3	89.8	−0.402	21.2	8.3
426	3	4.7	49.8	15.3	89.8	−0.402	30.3	8.3
427	3	0.8	23.9	4.7	49.8	−0.396	24.2	8.3
428	3	0.8	35.3	4.7	89.8	−0.36	29	13.9
429	3	0.8	67.8	49.8	89.8	−0.325	34.4	11.1
430	3	4.7	67.8	49.8	89.8	−0.325	29.4	5.6
431	3	15.3	67.8	49.8	89.8	−0.325	42.9	2.8
432	3	35.3	67.8	49.8	89.8	−0.325	52.9	5.6
433	3	23.9	67.8	49.8	89.8	−0.325	28.6	2.8
434	3	15.3	49.8	35.3	67.8	−0.324	29.4	5.6
435	3	0.8	35.3	23.9	49.8	−0.323	37.5	11.1
436	3	4.7	35.3	23.9	49.8	−0.323	29.4	5.6
437	3	15.3	35.3	23.9	49.8	−0.323	44.4	0
438	3	9	35.3	23.9	49.8	−0.323	32.4	5.6
439	3	2	35.3	23.9	49.8	−0.323	38.2	5.6
440	3	0.8	4.7	2	9	−0.322	32.4	5.6
441	3	4.7	23.9	15.3	35.3	−0.322	25.7	2.8
442	3	0.8	15.3	9	23.9	−0.32	35.5	13.9
443	3	4.7	15.3	9	23.9	−0.32	31.3	11.1
444	3	2	15.3	9	23.9	−0.32	53.1	11.1
445	3	0.8	49.8	23.9	89.8	−0.315	29.4	5.6
446	3	4.7	49.8	23.9	89.8	−0.315	30.3	8.3
447	3	15.3	49.8	23.9	89.8	−0.315	26.5	5.6
448	3	0.8	23.9	9	49.8	−0.31	44.4	0
449	3	4.7	23.9	9	49.8	−0.31	35.3	5.6
450	3	0.8	9	2	23.9	−0.308	36.4	8.3
451	3	0.8	35.3	9	89.8	−0.302	44.1	5.6
452	3	4.7	35.3	9	89.8	−0.302	33.3	8.3
453	3	0.8	15.3	2	49.8	−0.297	36.4	8.3
454	3	0.8	35.3	15.3	89.8	−0.229	33.3	8.3
455	3	4.7	35.3	15.3	89.8	−0.229	45.5	8.3
456	3	0.8	15.3	4.7	49.8	−0.225	51.4	2.8
457	3	0.8	49.8	35.3	89.8	−0.19	34.4	11.1
458	3	4.7	49.8	35.3	89.8	−0.19	30.3	8.3
459	3	15.3	49.8	35.3	89.8	−0.19	41.2	5.6
460	3	15.3	35.3	23.9	67.8	−0.189	44.1	5.6
461	3	4.7	35.3	23.9	67.8	−0.189	48.6	2.8
462	3	0.8	23.9	15.3	49.8	−0.188	41.9	13.9
463	3	4.7	23.9	15.3	49.8	−0.188	32.3	13.9
464	3	4.7	15.3	9	35.3	−0.187	54.5	8.3
465	3	0.8	9	4.7	23.9	−0.186	52.9	5.6
466	3	0.8	9	2	49.8	−0.174	38.7	13.9
467	3	0.8	35.3	23.9	89.8	−0.132	25.8	13.9
468	3	4.7	35.3	23.9	89.8	−0.132	51.4	2.8
469	3	15.3	35.3	23.9	89.8	−0.132	40.6	11.1
470	3	4.7	23.9	15.3	67.8	−0.131	51.6	13.9
471	3	0.8	15.3	9	49.8	−0.13	35.5	13.9
472	3	4.7	15.3	9	49.8	−0.13	34.4	11.1
473	3	0.8	4.7	2	23.9	−0.129	45.2	13.9

#	Stimulus type	Luminance					Left in front (%)	Canceled trials (%)
		a	*b*	*p*	*q*	ρ		
474	3	4.7	15.3	9	67.8	−0.099	36.7	16.7
475	3	0.8	9	4.7	49.8	−0.098	51.9	25
476	3	0.8	4.7	9	49.8	0.098	69	19.4
477	3	4.7	9	15.3	67.8	0.099	80.6	13.9
478	3	0.8	2	4.7	23.9	0.129	75	11.1
479	3	0.8	9	15.3	49.8	0.13	61.3	13.9
480	3	4.7	9	15.3	49.8	0.13	66.7	16.7
481	3	4.7	15.3	23.9	67.8	0.131	75.8	8.3
482	3	0.8	23.9	35.3	89.8	0.132	57.6	8.3
483	3	4.7	23.9	35.3	89.8	0.132	65.7	2.8
484	3	15.3	23.9	35.3	89.8	0.132	63.6	8.3
485	3	0.8	2	9	49.8	0.174	79.4	5.6
486	3	0.8	4.7	9	23.9	0.186	81.8	8.3
487	3	4.7	9	15.3	35.3	0.187	78.1	11.1
488	3	0.8	15.3	23.9	49.8	0.188	71.9	11.1
489	3	4.7	15.3	23.9	49.8	0.188	54.5	8.3
490	3	15.3	23.9	35.3	67.8	0.189	61.8	5.6
491	3	4.7	23.9	35.3	67.8	0.189	56.3	11.1
492	3	0.8	35.3	49.8	89.8	0.19	67.6	5.6
493	3	4.7	35.3	49.8	89.8	0.19	78.8	8.3
494	3	15.3	35.3	49.8	89.8	0.19	78.8	8.3
495	3	0.8	4.7	15.3	49.8	0.225	78.8	8.3
496	3	0.8	15.3	35.3	89.8	0.229	75.8	8.3
497	3	4.7	15.3	35.3	89.8	0.229	88.2	5.6
498	3	0.8	2	15.3	49.8	0.297	82.4	5.6
499	3	0.8	9	35.3	89.8	0.302	82.9	2.8
500	3	4.7	9	35.3	89.8	0.302	87.1	13.9
501	3	0.8	2	9	23.9	0.308	78.8	8.3
502	3	0.8	9	23.9	49.8	0.31	87.9	8.3
503	3	4.7	9	23.9	49.8	0.31	79.4	5.6
504	3	0.8	23.9	49.8	89.8	0.315	84.8	8.3
505	3	4.7	23.9	49.8	89.8	0.315	90.6	11.1
506	3	15.3	23.9	49.8	89.8	0.315	76.5	5.6
507	3	0.8	9	15.3	23.9	0.32	88.6	2.8
508	3	4.7	9	15.3	23.9	0.32	79.4	5.6
509	3	2	9	15.3	23.9	0.32	78.8	8.3
510	3	4.7	15.3	23.9	35.3	0.322	74.3	2.8
511	3	0.8	2	4.7	9	0.322	79.4	5.6
512	3	0.8	23.9	35.3	49.8	0.323	87.5	11.1
513	3	4.7	23.9	35.3	49.8	0.323	88.2	5.6
514	3	15.3	23.9	35.3	49.8	0.323	73.5	5.6
515	3	9	23.9	35.3	49.8	0.323	83.3	0
516	3	2	23.9	35.3	49.8	0.323	82.9	2.8
517	3	15.3	35.3	49.8	67.8	0.324	75	0
518	3	0.8	49.8	67.8	89.8	0.325	63.6	8.3
519	3	4.7	49.8	67.8	89.8	0.325	79.4	5.6
520	3	15.3	49.8	67.8	89.8	0.325	78.8	8.3
521	3	35.3	49.8	67.8	89.8	0.325	61.1	0
522	3	23.9	49.8	67.8	89.8	0.325	82.9	2.8
523	3	0.8	4.7	35.3	89.8	0.36	84.8	8.3
524	3	0.8	4.7	23.9	49.8	0.396	81.8	8.3
525	3	0.8	15.3	49.8	89.8	0.402	85.7	2.8
526	3	4.7	15.3	49.8	89.8	0.402	74.3	2.8

#	Stimulus type	Luminance					Left in front (%)	Canceled trials (%)
		a	*b*	*p*	*q*	ρ		
527	3	0.8	2	35.3	89.8	0.406	75	11.1
528	3	0.8	2	23.9	49.8	0.459	94.1	5.6
529	3	0.8	9	49.8	89.8	0.466	81.8	8.3
530	3	4.7	9	49.8	89.8	0.466	75.8	8.3
531	3	0.8	4.7	15.3	23.9	0.478	85.7	2.8
532	3	0.8	15.3	35.3	49.8	0.482	91.4	2.8
533	3	4.7	15.3	35.3	49.8	0.482	85.7	2.8
534	3	4.7	15.3	23.9	29.4	0.482	73.5	5.6
535	3	0.8	35.3	67.8	89.8	0.485	86.1	0
536	3	4.7	35.3	67.8	89.8	0.485	91.2	5.6
537	3	15.3	35.3	67.8	89.8	0.485	74.3	2.8
538	3	15.3	35.3	49.8	58.4	0.49	80	2.8
539	3	4.7	9	15.3	19.2	0.493	73.5	5.6
540	3	15.3	23.9	35.3	42	0.497	68.6	2.8
541	3	4.7	23.9	35.3	42	0.497	87.1	13.9
542	3	0.8	4.7	49.8	89.8	0.515	91.2	5.6
543	3	0.8	2	49.8	89.8	0.553	75.8	8.3
544	3	0.8	2	15.3	23.9	0.572	77.8	0
545	3	0.8	9	35.3	49.8	0.576	85.7	2.8
546	3	4.7	9	35.3	49.8	0.576	87.9	8.3
547	3	0.8	23.9	67.8	89.8	0.58	88.6	2.8
548	3	4.7	23.9	67.8	89.8	0.58	88.9	0
549	3	15.3	23.9	67.8	89.8	0.58	85.3	5.6
550	3	0.8	4.7	35.3	49.8	0.637	85.7	2.8
551	3	0.8	15.3	67.8	89.8	0.643	91.2	5.6
552	3	4.7	15.3	67.8	89.8	0.643	94.4	0
553	3	0.8	2	35.3	49.8	0.681	91.4	2.8
554	3	0.8	9	67.8	89.8	0.687	91.7	0
555	3	4.7	9	67.8	89.8	0.687	86.1	0
556	3	15.3	35.3	49.8	53.3	0.696	91.4	2.8
557	3	15.3	23.9	35.3	38	0.7	79.4	5.6
558	3	4.7	23.8	35.3	38	0.7	85.3	5.6
559	3	4.7	9	15.3	16.9	0.701	88.6	2.8
560	3	4.7	15.3	23.9	25.9	0.716	94.3	2.8
561	3	0.8	4.7	67.8	89.8	0.719	88.6	2.8
562	3	0.8	2	67.8	89.8	0.744	85.7	2.8

Table 5. Stimulus patterns tested in the experiment. The second column shows the stimulus type defined in Figure 4. Stimuli 1 through 180 belong to Type 1, stimuli 181 through 388 belong to Type 2, and stimuli 389 through 562 belong to Type 3. Luminance patterns of the stimuli are shown in columns three through six (*a*, *b*, *p*, *q*). In the table, luminance levels are normalized to a range between zero and 100. The maximum luminance was 89.2 cd/m^2. The seventh column shows *p* (Equation 10) calculated based on lightness. (Here, lightness was calculated by Equation 11 with $n = 0.46$.) The eighth and ninth columns show the percentages of ''left in front'' responses and the percentages of canceled trials, respectively.